SELF-PROPELLED ROTARY TOOL FOR TURNING DIFFICULT-TO-CUT MATERIALS

by

Grant Parker

B.Eng, University of Ontario Institute of Technology, 2009

A Thesis Submitted in Partial Fulfillment of the
Requirements for the Degree of

Master of Applied Science in Engineering

in the Graduate Academic Unit of Automotive Engineering

April 2011

University of Ontario Institute of Technology

ABSTRACT

Hard turning of difficult-to-cut materials is an economical method of machining components with high surface quality and mechanical performance. Conventionally in the machining industry, generating a component from raw goods includes a casting or forging process, rough machining, heat treatment to a desired hardness, and then finished-machining through a grinding process. Given the relative disadvantages of grinding, which include high specific energy consumption and low material removal rates, a newer technology has been introduced; hard turning. After the heat treatment of a cast part (generally in a range of 50-65 HRC), hard turning allows for immediate finished-machining. Hard turning reduces the production time, sequence, cost, and energy consumed. In addition, dry machining offsets environmental concerns associated with the use of coolant in grinding operations as well as other common turning operations.

Higher specific forces and temperatures in the contact area between the tool and workpiece lead to excessive tool wear. Generated tool wear affects the quality of the machined surface. Therefore, minimizing tool wear and consequently the generated surface quality become the status quo. Adverse effects associated with generated heat at the tool tip can be reduced by using

cutting fluid or by continuously providing a fresh cutting edge. The latter method will be applied in this thesis.

Rotary tool cutting involves a tool in the form of a disk that rotates about its axis. Different types of rotary tools have been developed, all with similar functional characteristics, however few are commercially available. Rotary tools can be classified as either driven or self-propelled. The former is provided rotational motion by an external source while the latter is rotated by the chip flow over the rake face of the tool.

A prototype self-propelled rotary tool (SPRT) for hard turning was developed which provides economical benefits and affordability for the user. It was tested on a turret-type CNC lathe by machining AISI 4140 Steel that was heat treated to 54-56HRC and Grade 5 Titanium (Ti-6Al-4V). Carbide inserts with ISO designation RCMT 09 T3 00 (9.5mm diameter) were used during machining. Both the SPRT rotational speed and the workpiece surface roughness were measured. Also, chips were collected and analyzed for each of the cutting conditions. The same procedure was followed during machining with the same tool which was denied the ability to rotate, therefore simulating a fixed tool with identical cutting conditions. Comparisons were made between tool life, surface roughness, and chip formation for the fixed tool and SPRT. Tool rotational speed was also analyzed for the SPRT. In general, the designed and prototyped SPRT showed very good performance and validated the advantages of self-propelled rotary tools.

A typical automotive component that is hard turned from difficult-to-cut materials is a transmission input shaft. These components demand high strength and wear resistance as they couple the vehicle's engine power to the transmission and remaining driveline.

ACKNOWLEDGEMENTS

The author graciously appreciates the encouragement and helpful advice provided throughout the development of this work by his supervisor Dr. H. Kishawy, and for the financial support provided through NSERC funding. Sincere appreciation is also expressed to the Faculty of Engineering and Applied Science at the University of Ontario Institute of Technology for the use of their manufacturing facilities and resources.

In addition, the author would also like to thank Mr. Hansen of Kennametal® for the donations of cutting inserts. A tremendous amount of gratitude is also expressed towards Mr. Kopp, who without his skill and ability would not have made it possible for the successful manufacturing of the prototyped self-propelled rotary tool. The author would also like to thank Mr. Pang and Mr. Hosseini for their assistance and recommendations during experimental testing.

TABLE OF CONTENTS

CHAPTER 3 EXPERIMENTAL SETUP

CHAPTER 4 RESULTS AND DISCUSSION

CHAPTER 5 CONCLUSIONS & FUTURE WORK

APPENDIX

LIST OF FIGURES

Figure **Page**

LIST OF TABLES

Table **Page**

NOMENCLATURE

b:	worn cutting tool edge length farthest away from the tool corner
C:	material constant
C_e:	tool cutting edge angle
C_{e1}:	tool minor (end) cutting edge angle
d:	depth of cut
f:	feed
F:	resultant shear force at the tool-chip interface
F_C:	cutting force
F_n:	force component normal to the shear plane
F_S:	shear force in the cutting velocity direction
F_T:	thrust force
F_u:	friction force along the rake face
F_v:	normal force to the rake face
i:	inclination angle; workpiece relative angle in the machine coordinate system
i_s:	inclination angle; workpiece absolute angle in rotary cutting
K_1:	material constant
KT:	crater depth
L:	overall workpiece length
n:	strain-hardening index
N:	normal force component at the tool-chip interface
P_f:	working plane
P_n:	cutting edge normal plane
P_o:	orthogonal plane
P_p:	tool back plane
P_r:	reference plane
P_s:	tool cutting edge plane
R:	resultant force at the deformation zone
r:	chip thickness ratio
T:	tool life
t_1:	undeformed chip thickness
t_2:	deformed chip thickness

V, V_c:	cutting velocity
VB_B:	flank wear land width
V_C:	chip velocity
V_{cr}:	relative chip flow velocity
v_f:	direction of cutting feed line
V_r:	rotating tool tangential velocity
V_S:	shear velocity
V_w:	workpiece velocity
V_{wr}:	workpiece relative cutting velocity
α_f:	rake angle measured in the p_f plane
α_n:	rake angle measured in the p_n plane
α_o:	rake angle measured in the p_o plane
α_p:	rake angle measured in the p_p plane
β_a:	friction angle
γ_f:	flank angle measured in the p_f plane
γ_n:	flank angle measured in the p_n plane
γ_o:	flank angle measured in the p_o plane
γ_p:	flank angle measured in the p_p plane
η:	chip flow angle in conventional cutting; relative chip flow angle in rotary cutting
λ:	friction angle
σ:	normal stress acting on the shear plane
τ:	shear stress
τ_0:	material constant
Φ , φ:	shear angle
φ_n:	normal shear angle
ψ:	tool approach angle

CHAPTER 1

INTRODUCTION

1.1 Motivation and Background

More than two-thirds of all the superalloys produced are consumed by the aerospace and automotive industries. The remaining portion of superalloy consumption is used by the chemical, medical, and structural industries in applications requiring high temperature properties and/or exceptional corrosion resistance. The ability to retain high mechanical and chemical properties at elevated temperatures make superalloys ideal for use in both rotating and stationary components in the IC engine of an automobile or in the hot end of a jet engine. These materials as well as structural ceramics and hardened steels pose formidable challenges for cutting tool materials during machining; hence they are referred to as difficult-to-cut. Typically, cutting tool material hardness of at least three times harder than the work material is recommended. Cutting materials such as ceramic and polycrystalline cubic boron nitride (PCBN) are recommended for turning hardened steel because of their ability to sustain the high temperature generated during the metal removal process. Hard turning with ceramic cutting tools has been a time proven manufacturing process that may replace some grinding applications.

High cutting temperatures are generated during hard turning. The generated temperatures cause thermal softening of the workpiece material in the cutting zone leading to reduced cutting forces. The reduction of generated force is desirable. However, excessive temperatures generate thermal damage on the machined surface as well as soften the cutting edge leading to plastic deformation. The high specific forces and temperatures affect the modes of tool wear in hard turning. The generated tool wear affects the integrity of the generated surface and therefore controlling it is a major challenge. The adverse effect of heat on the tool tip can be reduced by using cutting fluid or by continuously supplying a fresh cutting edge, as is the case in rotary cutting tools.

The basic difference between rotary cutting and conventional cutting is the movement of the cutting edge in addition to the main cutting and feed motions. Self-propelled rotary tools (SPRT) employ round inserts that rotate continuously about their central axis as a result of the driving motion impacted by the cutting force, thus minimizing the effect of thermal energy along the entire edge and preventing excessive heating of a particular portion of the cutting insert. Major benefits provided by rotary cutting tools include several hundred-fold increase in tool life, lower cutting temperatures, higher metal removal rates, generation of fine surface finishes due to the circular cutting edge, and improved machinability of difficult-to-cut materials such as nickel and titanium based alloys. Extremely low rate of flank wear can be obtained when machining superalloys, especially titanium alloys, even at higher speed conditions with very negligible or no effect on the machined surfaces.

Current commercially available self-propelled rotary tools are limited and only two companies supply them to the industry.

1.2 Scope of the Work

Although the economical benefits of machining with self-propelled rotary tools are very clear and any machinist would be more than willing to use such tools, the currently available SPRTs for hard-turning hinder their wide spread use in smaller machining facilities due to the initial capital investments and those in the continued use. Both manufacturers of rotary tools, who are Rotary Technologies © and Mitsubishi©, require specifically designed components and inserts for their production SPRTs for hard turning applications.

In this investigation, a self-propelled rotary tool for hard turning is designed, prototyped, and tested. The designed intent of the tool is to validate and achieve the benefits of rotary tools, while also providing the additional benefit through economical construction with 'off-the-shelf' parts. That is, all serviceable components are readily available in the industrial market, which includes bearings, washers, nuts, screws, and cutting inserts. The design is also machinist-friendly given its simplistic assembly and flexibility.

Results from hard turning with the designed and prototyped tool are presented and compared with those of a fixed tool with identical tool configuration. The factors monitored were tool wear, tool speed, surface

roughness, and chip formation under different cutting conditions and with difficult-to-cut workpiece materials.

CHAPTER 2

LITERATURE REVIEW & BACKGROUND

Machining by turning basically generates cylindrical forms with a single point tool. The cutting tool remains stationary while the workpiece rotates. This process is one of the most straightforward metal cutting methods with relatively uncomplicated definitions. However, being one of the most widely used machining methods, turning has become a highly optimized process. To maintain high efficiency requires the thorough appraisal of the various factors involved in applications.

2.1 Orthogonal and Oblique Cutting

Both orthogonal and oblique cutting are the two most fundamental and conventional machining types. The straight cutting edge on the tool used in orthogonal cutting is positioned normal to the cutting velocity direction. The depth of cut that the cutting edge engages into the workpiece is referred to as the chip thickness '*t*', as labeled, along with others, in Figure 2.1(a) below. Conventional oblique cutting is similar to conventional orthogonal cutting with the exception of the straight cutting edge being inclined with an acute angle from the cutting velocity direction. This acute angle is referred to as the inclination angle,

'*i*' and similar to conventional orthogonal cutting, the tool cutting edge is engaged into the workpiece at a depth of cut 't'. Figure 2.1(b) illustrates conventional oblique cutting.

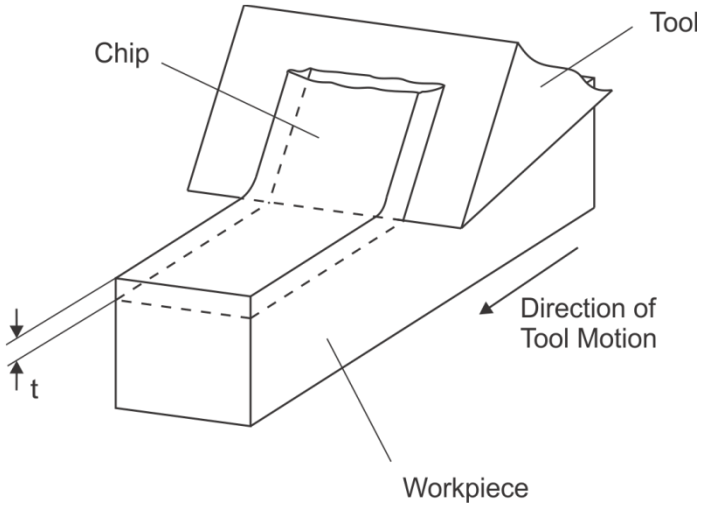

(a) Conventional Orthogonal Cutting

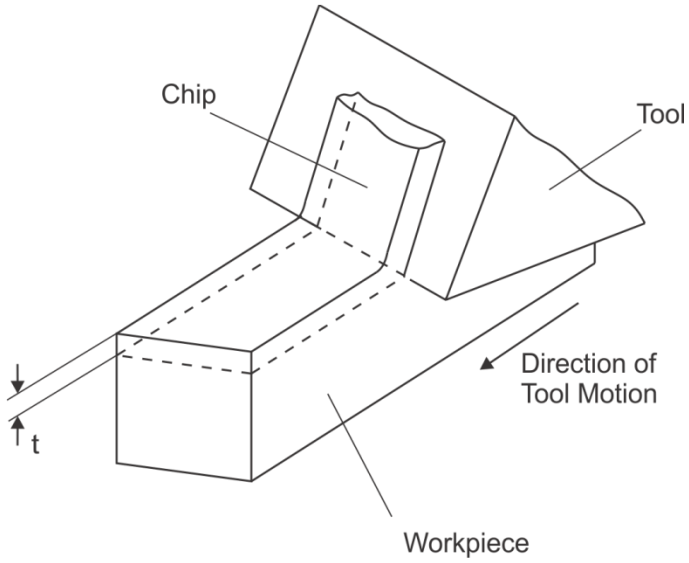

(b) Conventional Oblique Cutting

Figure 2.1 Two fundamental conventional cutting processes [1].

For orthogonal cutting, there are two basic cutting surfaces of the workpiece:

- The work surface: the surface of the workpiece to be removed by the machining process.
- The machined surface: the surface produced after the cutting tool passes.

One additional surface may be considered for many practical machining operations:

- The transient surface: the surface generated during cutting by the major cutting edge. This surface is always located between the work surface and machined surface, as shown in Figure 2.2.

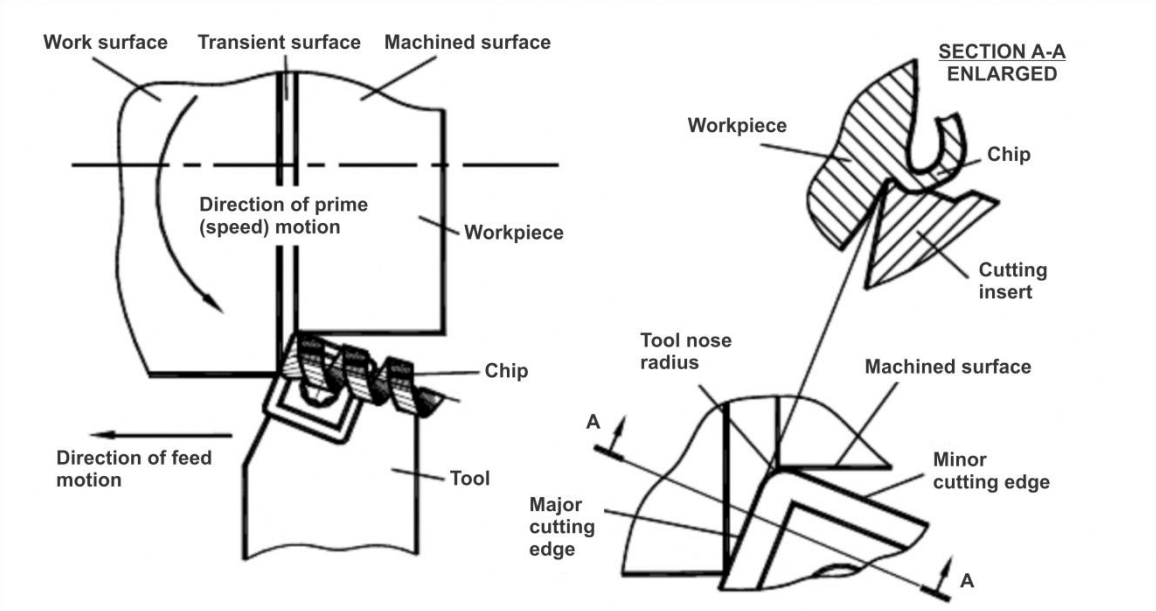

Figure 2.2 Turning terminology for workpiece surfaces [2].

This last surface distinguishes orthogonal cutting from other machining processes (i.e. shaping, planning, broaching, etc.) where the cutting edge is perpendicular to the cutting speed. As shown in Figure 2.2, the machined surface is generated from the tool nose and minor cutting edge, both of which directly affect the integrity of the machined surface including residual stresses and finish quality.

2.2 Tool Geometry

Depending on the geometry of the cutting tool, various mechanics, thermal reactions, and tool wear conditions will arise during cutting. There is a wide array of cutting tools for various cutting methods, such as turning, milling, drilling, broaching, and reaming. However, the lack of information on cutting tool geometry and its influence on the outcomes of machining operation can be explained as follows. In the past, benchmark findings on tool geometry were published when CNC grinding machines capable of duplicating any kind of tool geometry were not available and computers to calculate parameters of such geometry were not easily accessible. This made the task of reproducing proper tool geometries with manual machines very difficult. During the recent decades, the machining industry has seen several important changes that should bring cutting tool geometry to the forefront of tool design and implementation:

- Common practice for measuring the actual tool geometry of real cutting tools was a tedious and time-consuming process as no special equipment

besides toolmakers' microscopes were available. Currently, automated tool geometry inspection systems are available on the market.

- Typical modern tool grinders are CNC machine tools that accompany a four, five, or six axes setup. This makes tooling of extremely hard materials easier and allows for the generation of very complex geometries.
- Advanced cutting-insert manufacturing companies have now perfected production of inserts with very tight tolerances (using insert pressing technology such as spray drying).
- Modern machines used today have powerful rigid high-speed spindles, high-precision feed drives, and shrink-fit tool holders.

All of these improvements in the machining industry have pushed tool design, primarily including tool materials and geometry, to the vanguard as none of the traditional excuses for poor performance of cutting tools can be accepted.

In particular, the cutting tool geometry is of prime importance because it directly affects:

1. *Chip control.* Tool geometry defines the direction of chip flow. The direction is important to control chip breakage and evacuation.
2. *Productivity of machining.* The cutting feed per revolution is considered of the most major resources in increasing productivity. Feed can be significantly increased by adjusting to tool cutting edge angle. For example, milling utilizes this parameter to a large extent where it is found that increasing the lead angle to 45^{o} allows the feed rate to be increased

approximately 1.4-fold. As a result, a wiper insert is required to reduce feed marks left on the machined surface due to the increased feed rates.

3. *Tool life.* Cutting tool geometry directly affects tool life as this geometry defines the magnitude and direction of the cutting force and its components. These include the sliding velocity at the tool-chip interface, the distribution of thermal energy released in machining, the temperature distribution in the cutting edge, etc.
4. *The direction and magnitude of the cutting force and thus its components.* Four components of importance in the cutting tool geometry include the rake angle, the tool cutting edge angle, the tool minor cutting edge angle, and the inclination angle, all of which define the magnitudes of the orthogonal components of the cutting force.
5. *Quality (surface integrity and residual stress) of machining.* The comparison between tool geometry and the theoretical topography of the machined surface is common knowledge. Cutting geometry influences the machining residual stress which is realized when one recalls that the geometry defines to a great extent the state of stress in the deformation zone (i.e. around the tool).

The geometry of cutting tools, in particular the tool-in-hand tool geometry, has followed two basic standards: (a) the American National Standard B94.50-1975 “Basic Nomenclature and Definitions for Single-Point Cutting Tools 1”, reaffirmed date 2003, (b) ISO 3002/1 “Basic quantities in cutting and grinding –

Part 1: Geometry of the active part of cutting tools – General terms, reference systems, tool and working angles, chip breakers", second edition 1982-08-01. These standards have however failed to remain current and do not account for the significant changes in the machining industries and for the advances in metal cutting theory and practice, but they will be used here to outline the basic cutting tool geometry.

In cutting tool geometry (in particular for turning processes) there are a number of angles measured in various planes [3]. Figure 2.3 (which includes the tool-in-hand coordinate system) defines the main reference plane P_r, as perpendicular to the assumed direction of primary motion (the z-direction in the figure). The assumed direction of the cutting feed line, v_f, is also included along with the major cutting edge (1-2) and the minor cutting edge (1-3). This coordinate system also includes five basic planes which are defined relative to the reference plane P_r, some of which are included in the figure below [4].

- The working plane P_r contains the assumed feed motion direction and is positioned perpendicular to the main reference plane P_r.
- Perpendicular to P_r is the cutting edge plane P_s, which includes the major cutting edge (1-2 in Figure 2.3).
- Coincident with the *zy*-plane and therefore perpendicular to P_r and P_f is the tool back plane P_p (not included in Figure 2.3).
- The orthogonal plane P_o is perpendicular to the projection of the cutting edge onto the reference plane (illustrated in Figure 2.3 as directed through point 0' selected on the projection of the cutting edge).

- P_n is the cutting edge normal plane which is perpendicular to the cutting edge.

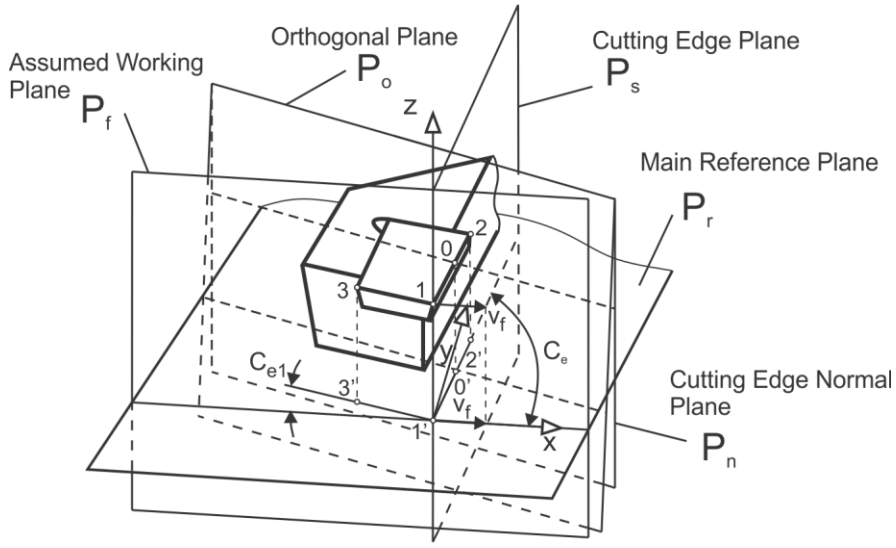

Figure 2.3 Reference planes in turning operations [5].

To further define the geometry of the cutting tool, a set of basic tool angles fall within the corresponding reference planes outlined in Figure 2.3. The definitions of these basic tool angles for the tool-in-hand coordinate system are as follows:

- Ψ is the tool approach angle; the acute angle that P_s makes with P_p and is measured in the reference plane as shown in Figure 2.4.
- Rake angle is the angle between the reference plane P_r, and the tool rake face. The rake angle is defined as the normal rake angle α_n if the angle is measured in the cutting edge normal plane P_n. Also, different rake angles α_f, α_p, *and* α_o are defined as shown in Figure 2.4.

- Flank angle is the angle between the tool cutting edge plane P_s and the tool flank face. Similarly, if the flank angle is measured in the cutting edge normal plane, the angle is referred to as the normal flank angle, γ_n. Different flank angles γ_f, γ_p, *and* γ_o are defined as shown in Figure 2.4.
- Orientation and inclination of the cutting edge are specified in the tool cutting edge plane P_s. In this plane, the cutting edge inclination angle i (or i_s) is the angle between the cutting edge and the reference plane.
- The tool cutting edge angle, C_e, is shown in Figure 2.4. This angle is defined as the acute angle that the tool cutting edge plane makes with the assumed working plane and is measured in the reference plane P_r. Also, the tool minor (end) cutting edge angle, C_{e1}, is the acute angle that the minor cutting edge plane makes with the assumed working plane and is measured in the reference plane P_r.

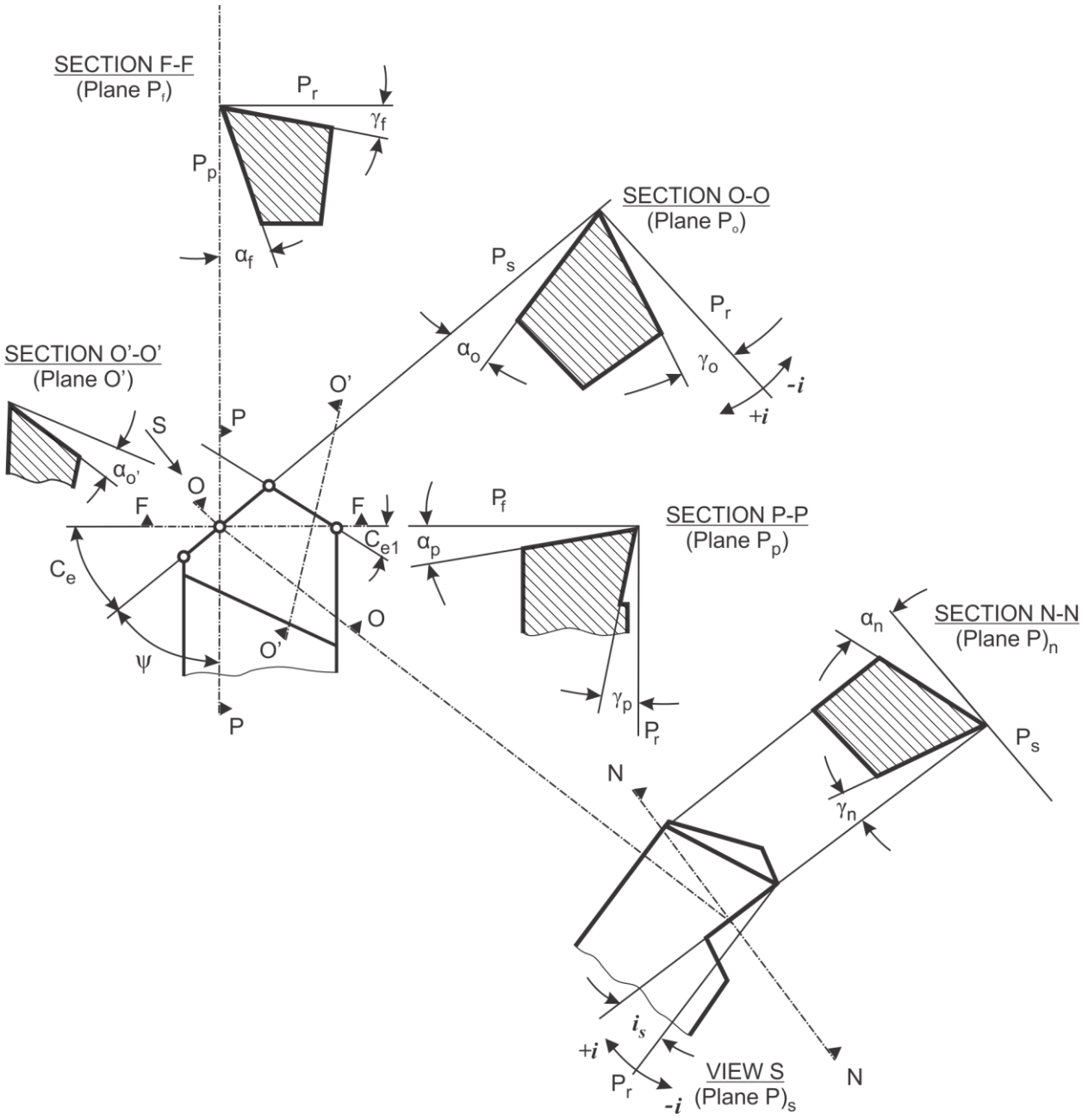

Figure 2.4 Tool angles for the tool-in-hand system [2].

The flank and rake angles are zero when the corresponding construction planes coincide. The measuring angles become positive when the generated angle produces a tool with less material in comparison to the definition of the zero

angles. For the tool approach angle, it is considered positive when directed in the clockwise direction.

2.2.1 System Considerations

There are three basic systems in which the tool geometry should be considered, namely, the tool-in-hand, tool-in-machine (holder) and tool-in-use geometry. Therefore, it should be appreciated that the necessity of such consideration would entail not only the understanding of the tool geometry as it appears on drawings or shown in catalogues of the tool manufacturers, but that it can be significantly altered through a wide range depending upon the tool holder used. That is, the resultant geometry can be considerably altered depending on the location of the tool in the machine relative to the workpiece.

2.2.2 Tool Angle Influence on Machining

As mentioned previously, there is a plethora of different angles that are inherent to the tool geometry which can also be translated and altered when coupled with the tool holder and workpiece. Some of these angles are important to elaborate on because of their influence during a machining operation, especially during turning.

The tool cutting edge angle affects the cutting process to a large degree since given a specific feed and cutting depth, it directly affects the uncut chip thickness as well as the chip width and therefore tool life. To expand, when C_e

decreases, the width of the chip increases as the active portion of the cutting edge also increases. As a result, there is an improvement in heat removal from the tool and therefore increased tool life. For example, in rough turning of carbon steels, a small change from 45^{o} to 30^{0} has lead to five-times improved tool life. There are however drawbacks, one of which includes an increase in the radial cutting force component, which can result in reduced accuracy and stability of machining especially if the tool holder and the workpiece fixture cannot withstand the increased load [5].

The tool rake angle also has a significant impact during the cutting process. The rake angle can be measured as positive, negative, or zero (also referred to as neutral). Generally, an increase in the rake angle reduces machining horsepower consumed per unit volume of the current workpiece layer being removed at a rate of approximately 1% per degree starting from $\alpha = -20^{o}$. This results in reductions in both the cutting force and tool-chip contact temperature. So, it would seem that a high positive rake angle would be ideal for practical machining. Application, however, indicates there are a number of drawbacks of increasing the rake angle. The largest impact is that the cutting tool tip loses strength as the rake angle increases (increased removal of tool material). The normal force that acts on the tool-chip interface causes bending of the cutting tool tip which results in weakened tool strength followed by tool chipping. Also, the tool-chip interface contact area diminishes with the rake angle which shifts the normal force closer to the cutting edge, however, when cutting with a negative rake angle, the normal force causes compression of the

tool material. Since tool materials tend to have very high compressive strength, the cutting edge strength is much higher and can survive. In addition, an increased rake angle also shifts the maximum contact temperature at the tool-chip interface closer to the cutting edge which decreases the tool life as discovered by Astakhov [6]. The rake angle is not an independent variable as it is also affected by the tool holder and not just the cutting tool insert geometry. Further, application of chip breakers often dictates the resulting rake angle rather than other parameters of the cutting process such as power consumption, cutting force, and tool life.

Flank angle also has a large impact on the tool life. If the flank angle $\gamma=0^{\circ}$ then the flank surface is contacting the workpiece surface. Due to the phenomenon of spring-back of the workpiece material, there is an increased frictional force developed on the touching surfaces which eventually leads to tool breakage. Therefore, the flank angle affects cutting performance by decreasing the rubbing on the tool's flank surfaces. Also, as the flank angle increases, more material is removed from the cutting tool insert and the strength of the adjacent cutting edge as well as the heat dissipation of the tool is significantly reduced. Both of these factors result in decreased tool life. However, an advantage of an increased flank angle includes a decreased cutting edge radius which results in reduced frictional and deformation components of the flank force (more noticeable with small feeds). This generates less heat and therefore increases tool life.

2.3 Tool Materials

Several tool materials exist in the metalworking industry today, which include high-carbon steels, ceramics, and diamonds. It is important to note the differences between the tool materials and how each type is best suited for a particular application. The three most significant properties of a tool material are:

- *Hardness*: a resistance to the penetration of an indenter. This property directly correlates to the strength of the cutting tool material [7]. If a tool material is able to maintain high hardness at elevated temperatures, it is referred to as 'hot hardness'. Figure 2.5 below, illustrates the various hardness capabilities of materials with change in temperature.
- *Toughness*: the ability of a material to absorb energy up until the point of fracture. The higher the fracture toughness, the greater the resistance to shock loading, chipping and fracturing, vibration, runouts, and other sources of imperfections in the machining system. Figure 2.5 illustrates that for tool materials, hardness and toughness change in opposite directions; thus a market trend has been to develop tool materials that have increased toughness with maintained hardness.
- *Wear Resistance*: the point of reaching acceptable tool life before tools are replaced; a characteristic that is the least understood.

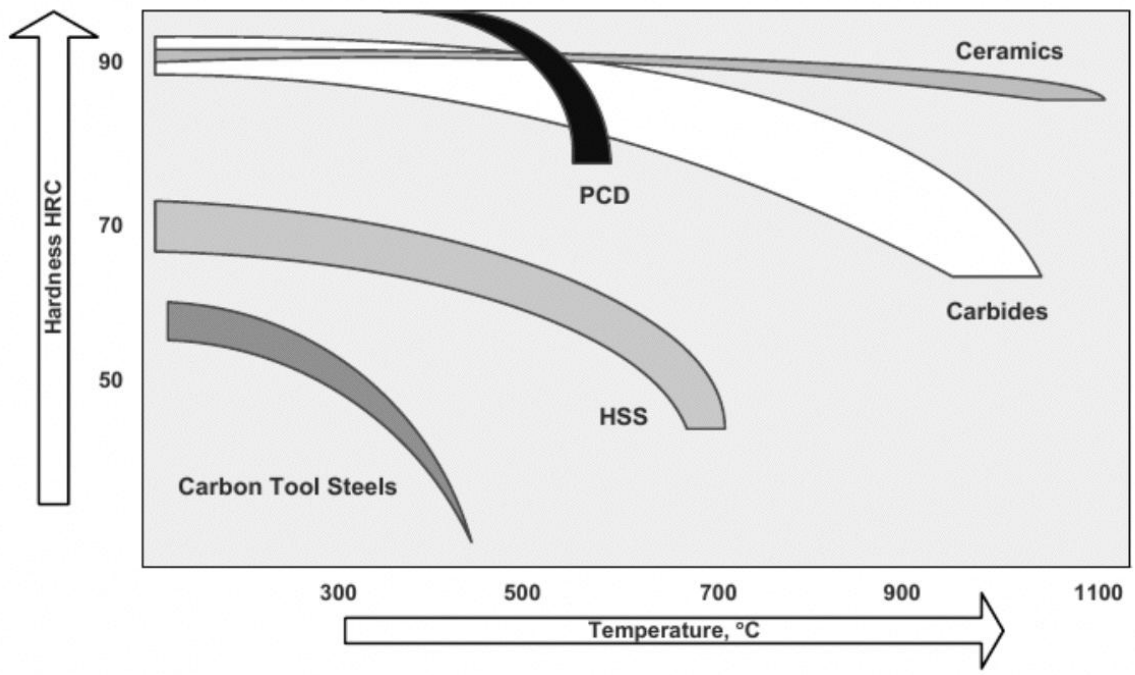

Figure 2.5 Hardness of tool materials versus temperature [7].

To be precise, wear resistance is not a true characteristic of tool materials. The nature of tool wear is yet to be clearly defined, given the numerous theoretical and experimental studies conducted. Metalworking tool wear is the result of a complicated combination of physical, chemical, and thermo-mechanical phenomena. Due to the various mechanisms of wear (i.e. abrasion, adhesion, diffusion, oxidation, etc.) acting simultaneously, it is difficult to identify the dominant mode of wear, and therefore provide the optimal defense. An experimental device used by tool material manufacturers to characterize wear resistance is pin-on-disk tribometer, however, as discussed by Astakhov [6], both the method and results are considered unacceptable.

There are a number of different tool materials available today; five important groups will be described in this section: carbides, ceramics, polycrystalline cubic boron nitrides (PCBNs), polycrystalline diamonds (PCDs), and solid or thick film diamond (SFDs or TFDs).

2.3.1 Carbides

The carbide cutting tool materials on the market today include compositions of silicone and titanium carbides (also known as cerments), as well as tungsten carbides and other compounds of a metal (such as Ti, W, Cr, Zr) or metalloid (B, Si) and carbon. A large advantage of carbides is that they have excellent wear resistance and high hot hardness. Typically, a carbide cutting tool consists of carbide particles bound together in a cobalt matrix by a sintering process. The amount of cobalt significantly affects the properties of the carbide cutting insert. As the cobalt content increases (from a range of 3-20%) the toughness of the cutting insert increases while its hardness and strength decrease. Metal cutting productivity can be increased substantially without sacrificing insert wear resistance if the insert is combined with special coating materials and is layered in a particular sequence.

2.3.1.1 Carbide Coatings: Selecting the optimum grade of carbide material for a cutting insert has become quite the dilemma for the metalworking industry due to the plethora of grades, coatings, coolants, and cutting conditions which vary from workpiece to workpiece. As a result, most cutting tool manufacturers offer a guide for the initial selection of carbide grade for the desired cutting insert based on the cutting conditions.

Once the carbide grade has been selected, a thin-film hard coating and/or thermal diffusion process can be considered. Currently, 85% of carbide tools and 40% of super-hard tools used in the metalworking industry are coated [6]. The carbide materials provide excellent substrates for coatings such as TiN, TiAlN, TiCN, solid lubricant coatings, and multilayer coatings. Coatings provide improved tool life and increase the performance of carbide tools in high-productivity, high-speed and feed cutting conditions, dry machining, and the machining of difficult-to-cut materials. In detail, the benefits of coatings are:

- Increased surface hardness for greater wear resistance.
- Increased resistance to abrasion, adhesion, flank, and crater wear.
- Reduced coefficient of friction to allow increased chip sliding and thus reduce cutting forces, prevent adhesion to the contact surfaces, and reduce heat generated due to chip sliding.
- Reduced absorption of thermal energy into the tool.
- Increased corrosion and oxidation resistance.
- Improved surface quality of finished parts.

The most common coatings for carbides applied in single or multi-layers are described in Table 2.1 below. In an attempt to correlate the coating materials and their performance, Klocke and Krieg discovered there are four basic groups of coatings on the market [8]. These include titanium based coating materials where the metallic phase is often supplemented with metals such as Al and Cr, which are added to improve particular properties such as hardness or oxidation resistance. These types of coatings and those included in Table 2.1 are basic physical vapor deposition (PVD) coatings.

Table 2.1 Common Carbide Coatings [8].

Coatings	Characteristics
Titanium Nitride, TiN	Gold-coloured coating provides excellent wear resistance with a wide range of workpiece materials and allows for higher feed and cutting speeds. Applications in forming processes will result in a decrease in galling and welding of workpiece material with an improvement in surface finish of the formed component. Tool life increase on the order of 200-300%, however, has seen as high as 800%.
Titanium Carbonitride, TiCN	Bronze-coloured provides improved wear resistance in abrasion, adhesion or difficult-to-cut materials such as cast iron, alloys, tool steels, copper (and its alloys) and titanium alloys. Similar to TiN, feed and cutting speeds can be increased and tool life can

	improve on the order of 800%. Improved forming operations of abrasive materials over those formed with TiN.
Titanium Aluminum Nitride, TiAlN	Purple-black in colour, TiAlN is a coating which excels at machining of abrasive and difficult-to-machine materials such as cast iron, aluminum alloys, tool steels, and nickel alloys. TiAlN offers improved ductility which provides the option for interrupted operations. Excellent oxidation resistance provides unparalleled performance in high-temperature machining processes.
Chromium Nitride, CrN	Silver-coloured, CrN provides high-thermal stability, which in turn helps in the aluminum die casting and deep-draw applications. Also reduces built-up-edge production commonly associated with machining titanium alloys with Ti-based coatings.

2.3.2 Ceramics

Ceramic tool materials are composed primarily of fine grained aluminum oxide, cold-pressed into the desired insert geometry and sintered under high pressure and temperature. White ceramics refer to pure aluminum oxide ceramics while the addition of titanium or zirconium oxide results in black cermets (not related to carbide cermets as mentioned earlier). Aluminum oxide ceramics are brittle and primarily used for hardened steels. Another form of ceramic cutting material is silicon nitride which is relatively soft and tough and used for cast irons. Typically the higher proportion of aluminum results in a

harder material whereas the higher proportion of silicon nitride results in a tougher material.

Ceramics provide high hardness with abrasive wear resistance at elevated temperatures, as shown in Figure 2.5. As tool inserts become hotter, they typically become softer, however, ceramics react at a much slower rate because of the lack of metal content. Ceramic cutting materials also offer chemical stability inasmuch as they do not react with the workpiece material (i.e. no diffusion wear). This is a large downfall of carbide materials in high-speed machining processes. Ceramic cutting inserts are ideal for machining most ferrous materials as well as superalloys. For copper, brass and aluminum, ceramics should not be used due to the formation of built-up edge.

A large downfall of ceramics is the higher costs and brittleness. In an attempt to protect the cutting edges, a heavy edge preparation such as T-land (type of chamfering) or honed edge is implemented into the ceramic cutting insert. Coatings are not common with ceramic cutting inserts due to the high cost and weak adhesion between the coating materials and ceramic substrates.

There has been much improvement in tool wear with ceramic cutting inserts through the adoption of small grain sizes. In hard turning applications, ceramics cutting inserts have provided up to 20 times improved tool life.

2.3.3 Cubic Boron Nitride (CBN)

Using cubic boron nitride crystals, CBN inserts are created through sintering at very high-pressure and temperature with a binder and bonded to a tungsten carbide substrate. The binder (usually a metallic or ceramic matrix) provides the chemical stability which allows the polycrystalline cubic boron nitride (PCBN) to withstand the abuse in high-speed machining environments. High impact resistance is provided by the tungsten carbide substrate which allows for the depths of cuts and high speeds associated with machining of hardened ferrous materials. PCBN tools also offer the following benefits:

- Capable of machining hardened and heat-treated steels
- Excellent surface finishes that do not require further grinding
- High productivity rate that can exceed four times higher than that in grinding
- Excellent abrasion resistance; twice that of ceramics and ten times that of carbide
- Excellent heat dissipation and wear resistance

Part of the contribution to the high quality of cutting of PCBN tools is by cutting edge preparation. This can be applied as a small hone for finishing cast irons, or as a T-land for heavy roughing of white iron, or as a combination of these two preparations. The practice of applying a T-land to PCBN inserts used for cutting super-hard materials has been deemed necessary for extending tool life. However, this has become so widely accepted that it is rare to find a PCBN insert without any chamfering. It has been found that this type of edge

preparation actually produces suboptimal results and limits tool life and diminishes cutting performance. Further application of newer edge preparation alternatives are required to make a larger improvement to the tool life of these inserts for the super-hard materials that are increasing in popularity.

PCBN tools are commonly used for machining cast irons, sintered iron, superalloys, and hardened steels.

2.3.4 Polycrystalline Diamond (PCD)

Being one of the most versatile engineering materials in the world, diamond is the strongest and hardest known substrate with the highest thermal conductivity of any material at room temperature and low surface friction. To date, no other material, natural or man-made can match these unique properties [9].

PCD tools are manufactured using a layer of industrial crystals which consist of a mixture of graphite and a catalyst (typically nickel) under 7000 MPa of pressure and at a temperature of 1800°C, coated on a carbide substrate and further subjected to high-pressure and temperature (6000 MPa and 1400°C, respectively).

PCD tools can provide up to 500 times the abrasion resistance of most tungsten carbide tools and also provide high thermal conductivity. As a result, PCD tools have replaced many carbide, ceramics and natural diamond in many applications, ranging from turning, boring, milling, slotting and chamfering of a

plethora of materials. A substantial benefit of PCD tools is that their extended tool life and resulting increased productivity more than offsets the higher initial cost by lowering the unit cost of parts produced. Further, PCD tools can be re-sharpened after extended use. However, having high abrasion resistance and hardness, PCDs have relatively low toughness. To improve this downfall, structural changes have been implemented which includes the combination of different sized diamond particles which provides an increased packing density, resulting in higher adjacency of diamond grains. This enhances the chipping resistance of the cutting edge and also provides a smoother transition between the layers of the ground edge as opposed to the micro-serrated edge normally seen in most other PCD compositions.

2.4 Tool Wear

A large contribution to tool failure is tool wear. The failure of tools is most commonly believed to be premature failure (i.e. tool breakage) and by progressive tool wear. Figure 2.6 illustrates some types of failures and wear on cutting tool inserts.

Most often tool wear depends on tool geometry and material, workpiece materials, cutting parameters (i.e. cutting speed, feed rate and depth of cut), cutting fluids, and machine-tool characteristics.

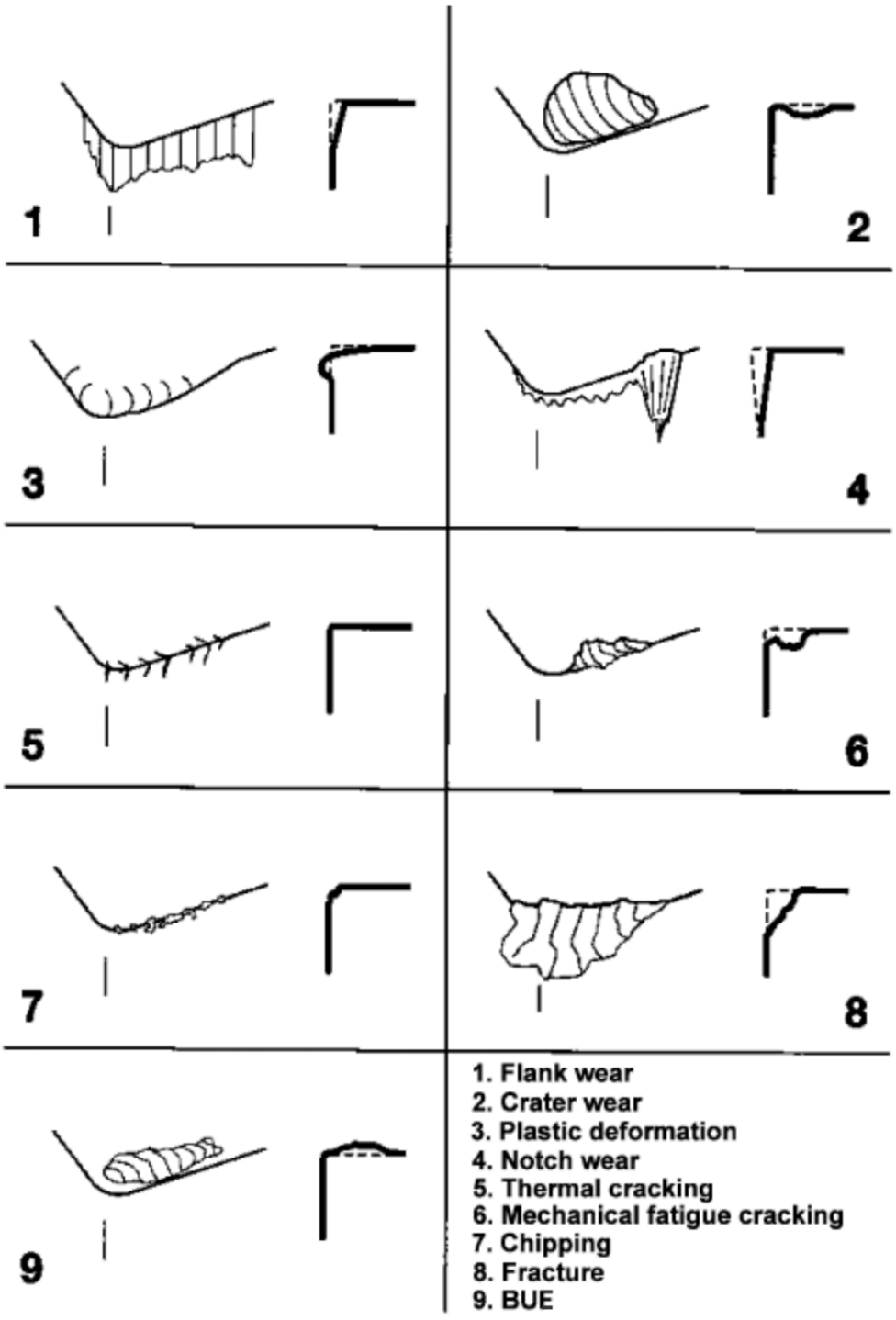

Figure 2.6 Types of tool wear on cutting tool inserts [10].

2.4.1 Types of Tool Wear

Typically tool wear is a gradual process and there are two basic and most important measured forms of wear zones in cutting tools: flank wear and crater wear. Flank wear is more closely monitored to determine the degree of tool wear. As shown by Figure 2.7, there are four regions divided along the cutting edge that are used as a standard for wear measurements (ISO 3685:1993) [11]; they are:

- Region C: curved portion of cutting edge at tool corner.
- Region B: is the remaining straight part of the cutting edge in zone C.
- Region A: is the quarter of the worn cutting edge length '*b*' farthest away from the tool corner.
- Region N: portion that extends beyond the area of mutual contact between the tool and workpiece for approximately 1-2mm along the main cutting edge; characteristic tool wear is notch type.

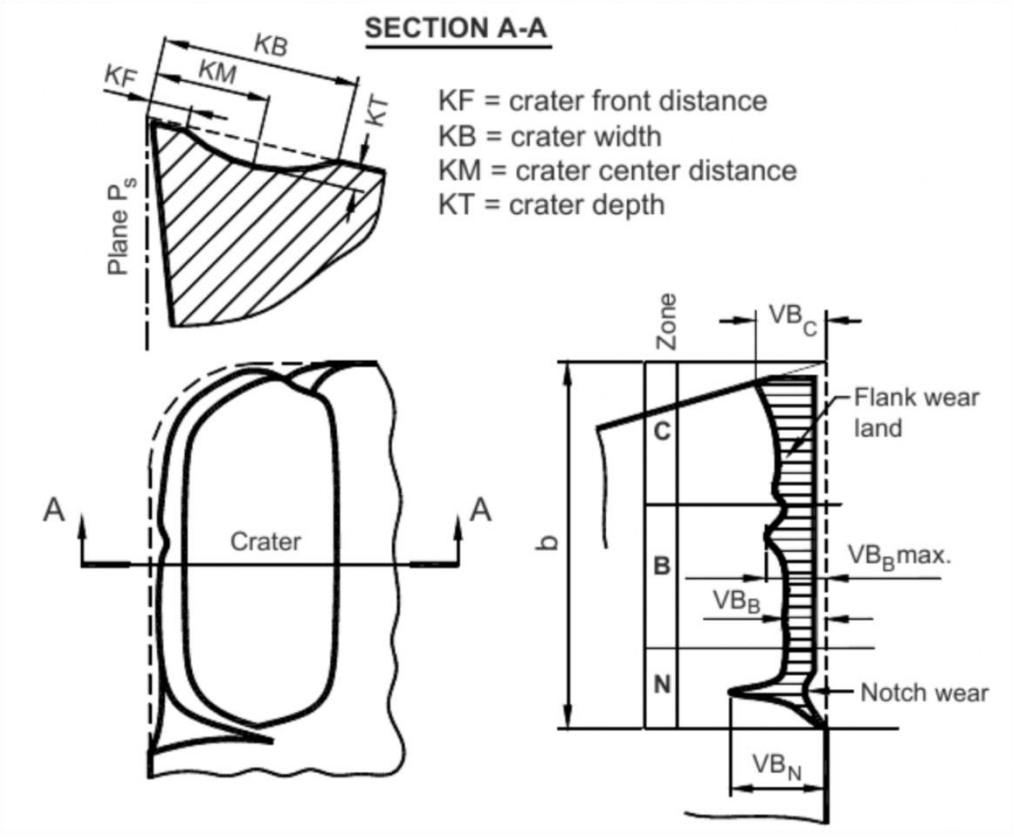

Figure 2.7 Types of tool wear according to standard ISO 3685:1993 [11].

The flank wear land width, VB_B, is measured within zone B in the cutting edge plane P_s (Figure 2.3 from before), perpendicular to the major cutting edge, and from the position of the original major cutting edge. The crater depth, *KT* is measured as a maximum distance between the crater cavity bottom and the original face in region B.

A toolmaker's microscope is most commonly used to measure tool wear or a stylus type instrument similar to a profilometer can be used.

2.4.2 Progression of Tool Wear

To illustrate the relationship between flank (rake) wear and cutting time, τ_m, or the overall workpiece length, L, tool wear curves can provide a comparison. As shown in Figure 2.8(a), the flank wear width progresses to a maximum VB_B after certain length of cutting. The progression in flank wear curves can be divided into three noticeable regions; the first region (region I in Figure 2.8(a)), is the result of the initial or primary wear. Here exists a high wear rate as the result of accelerated wear of the tool layers damaged during the manufacturing or re-sharpening of the cutting inserts. The adjacent region (region II in Figure 2.8(a)), withstands a steady rate of tool wear and is the normal operating region for the cutting insert. The last region (region III in Figure 2.8(a)), is an accelerated wear region where high cutting forces, temperatures, and severe tool vibrations occur, thus the tool should not be operated within this region. In the best interests of lowering tool wear, cutting speeds should be of prime concern. The relationship between these parameters is illustrated Figure 2.8(b), where there are three different cutting speeds (while maintaining all other cutting conditions), which are v_1, v_2, and v_3. Since v_3 is much higher than v_1 and v_2, it demonstrates a faster rate of tool wear. Once the tool wear reaches the maximum allowed wear, the tool has become worn out.

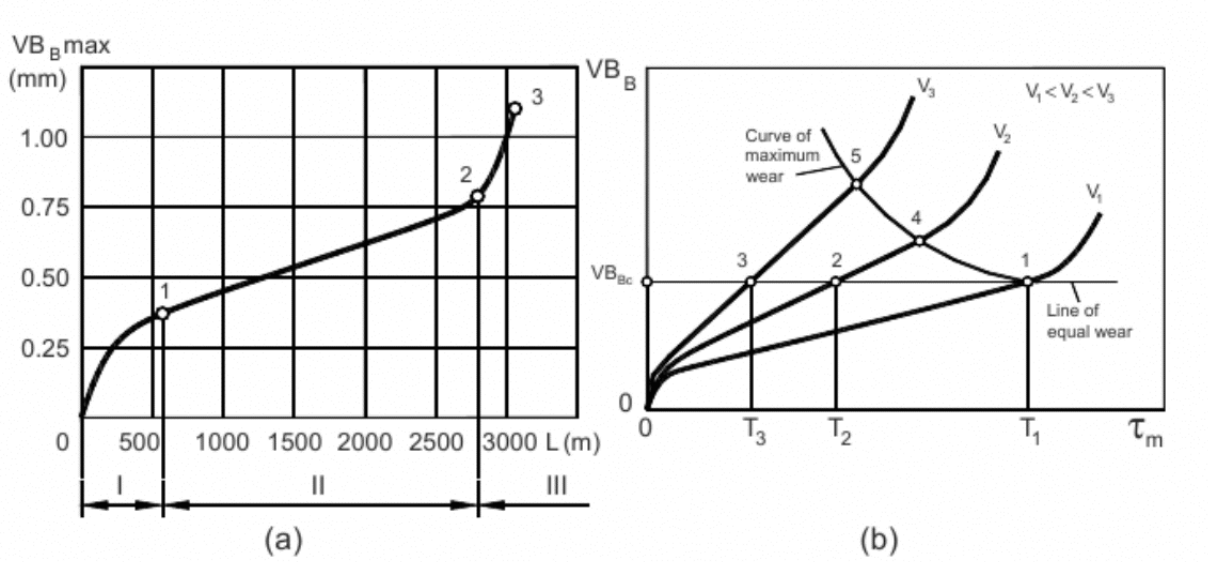

Figure 2.8 Wear curve types: (a) normal wear curve, (b) evolution of flank wear land VB_B as a function of cutting time for different cutting speeds [5].

During normal operation, VB_{Bc} is selected from a range of 0.15-1.00 mm depending upon the type of machining operation, the condition of the machine tool, and the quality requirements of the finished product. As shown in Figure 2.8(b), T_1 is the corresponding tool life to a cutting speed v_1, and similar matches for T_2, v_2, and T_3, v_3. If the integrity of the machined surface allows it, the curve of maximum wear instead of the line of equal wear should be used. Therefore, the range of tool life between lower and higher cutting speeds becomes less significant and a higher productivity rate can be achieved.

2.4.3 Tool Wear Mechanisms

There are several forms of mechanisms that cause tool wear, which are: abrasion, diffusion, oxidation, fatigue, and adhesion. These mechanisms can be described as follows:

1. *Abrasion*: Wear that occurs when hard particles (carried by the chip flow) abrade and remove tool material. Can also occur due to chip form or a chemical reaction between cutting fluids and chips (as with powdered metal steels which form powder chips), also called *erosive* wear. Abrasion primarily occurs on the flank surface of the tool, and thus is the main cause of flank wear, notch wear, and nose radius wear.
2. *Diffusion*: During wear by diffusion, a constituent of the tool material diffuses into a solid solution with the chip material, weakening the tool surface and results in a wear crater on the rake face of the tool. Diffusion wear rate depends primarily on the stability of the tool material in the work material and the contact time between tool and chip at elevated temperatures, and increases exponentially as the cutting temperature increases.
3. *Oxidation*: This wear mechanism occurs when constituents of the tool react with the atmospheric oxygen. Often occurs near the free surface of the part, where the tool-chip interface area with elevated temperature is exposed to the atmosphere. Oxidation wear can lead to severe notching of the tool and the debris or particles of work material may also result in the production of hard oxide particles which increase abrasive wear.

4. *Thermal Fatigue*: Thermal cycling and thermal shock can lead to early failure with PCBN tooling. This can be associated with both interrupted turning and milling (which by nature is interrupted). When machining with coolant, thermal shock of the cutting edge causes early tool chipping. This is associated with the rapid cooling and heating of the tool edge as it enters and exits the interruption, along with the rapid cooling which happens when coolant is applied.
5. *Adhesion*: One of the most significant types of wear at lower cutting speeds, adhesion occurs when small particles of the tool adhere or weld to the chip due to friction and are removed from the tool surface. Occurs on the rake face of the tool and contributes to the formation of crater wear. The rates of adhesion wear are generally low, thus this form of wear is not normally significant. However, at a particular point, significant adhesive wear can generate a built-up-edge (BUE), which can also lead to tool chipping.

2.5 Tool Life

One of the most important variables in machining, tool life must be properly gauged in order to ensure that considerable time is not lost if and when a tool is replaced and reset. Therefore, we can define tool life as the time a tool will cut to a desired level of quality and is expressed in minutes between changes of the cutting tool. Continued cutting past the tool life expectancy results in

further wear and ultimately failure of the cutting tool which increases the surface roughness and decreases the dimensional accuracy of the workpiece.

2.5.1 Taylor's Formula

Easily determined quantitatively, tool wear is most often used as a lifetime criterion. The flank wear land VB_B is often used as the criterion given its influence on the workpiece surface quality and accuracy. As shown by Figure 2.9, wear curves based on flank wear and cutting time are plotted for various cutting speeds as well as the tool life.

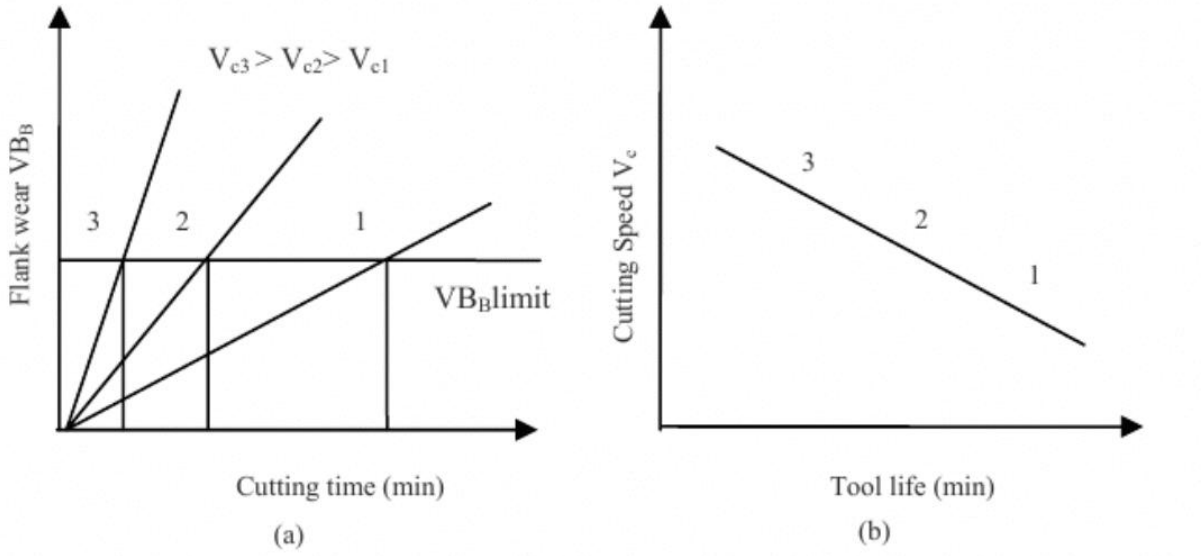

Figure 2.9 Wear curves for various cutting speeds (a), and tool life curves (b) [12].

As presented by Taylor [12], the following algebraic expression can be used to model tool life:

$$V_c T^n = C \tag{2.1}$$

where V_c is the cutting speed (m/min), T is the tool life (min) taken to develop a certain flank wear land (VB_B), n is an exponent that depends on the cutting parameters and C is a constant. At T = 1 min, C is equal to the speed. From the above formula and for each combination of tool material and workpiece and each cutting parameter, there is a distinct n and C value that is determined experimentally. Therefore, by data such as that shown in Figure 2.9, two points on a plot can be used to determine the values of n and C for a given cutting scenario and thus predict and expand on the expected tool life.

2.5.2 Modified Taylor's Tool Life Formula

From the above tool life formula, we can see that only the cutting speed is a parameter that affects the estimated tool life. This is the result of Taylor obtaining the formula through his work using high-carbon and high-speed steels as tool materials. Once carbides became a more common cutting material, it was found that both cutting feed and the depth of cut were also significant in determining the expected tool life. Therefore, Taylor's formula became modified and accommodates the newer revisions as follows:

$$V_c T^n f^a d^b = C \tag{2.2}$$

where *d* is the depth of cut (mm) and *f* is the feed (mm/rev). The exponents *a* and *b* are determined experimentally for each combination of the cutting conditions.

In summation, tool life depends on: cutting parameters (as listed above); tool material and geometry; type and condition of cutting fluid used; workpiece material (i.e. chemical composition, hardness, strength, toughness, homogeneity and inclusions); and the machining operation. Therefore, it makes for a very difficult task to develop a universal tool life criterion.

2.6 Mechanics of Metal Cutting

By understanding the mechanics of chip formation during machining will assist in providing the basis for prediction of the various interactions taking place. This includes deformations, temperatures and forces as they determine the quality of the machining process and finished product. For example, high temperatures in the cutting region would result in softening of the workpiece material which will affect the cutting forces. However, high cutting temperatures will be detrimental to the cutting tool material. The cutting forces will determine the machine tool power requirements and the loads transferred to the tool's packaged bearing assemblies as well as any deflections of the workpiece, cutting tool, fixture, and machine tool structure. Cutting tool geometry plays a large role in both cutting temperatures and forces generated during a machining process. In addition, cutting speed, feed, and depth of cut have significant influence on cutting forces generated. As a result, an understanding of what is happening

during the metal removal process is necessary for the study of machining mechanics as well as for successful tool design construction.

Chips formed can be classified into three different groups: discontinuous chips, continuous chips, and continuous chips with built-up edge (BUE) [13]. Factors such as tool geometry, workpiece material properties, tool material properties, and cutting parameters affect the formation of chips. Discontinuous chips are formed during machining of brittle materials at low cutting speeds, in addition to large undeformed chip thickness and small to negative rake angles. Continuous chips are formed when machining with ductile materials at high cutting speeds with small-undeformed chip thickness, large rake angles, and appropriate coolant. Continuous chips with BUE are formed during the machining of workpiece materials that have strong adhesion with the cutting tool material, large undeformed chip thickness, and small rake angles. Both discontinuous and continuous with BUE chip formations are undesirable since fluctuating forces are generated which result in poor surface quality and dimensional accuracy. Stable force generation follows from the formation of continuous chips and thus develops a final product with better surface quality and dimensional accuracy.

2.6.1 Merchant's Model of Fundamental Mechanics of Orthogonal Metal Cutting

To gain a fundamental understanding of the forces involved during the metal removal process, Merchant's model illustrates the relations at the shear zone and the tool-chip interface. It follows the concept of a thin primary deformation zone model for the orthogonal cutting process. It is assumed that the workpiece is an ideal perfectly rigid plastic material. In addition, the following assumptions are also made [2]:

1. Continuous chips without BUE are formed.
2. Cutting velocity is held constant.
3. The cutting tool has a sharp cutting edge and there are no flank face interactions.
4. The chip is considered to remain in stable equilibrium under the counteraction of resultant forces in the shear zone and tool-chip interface.

As shown in Figure 2.10 below, the fundamental orthogonal cutting forces can be simplified in representation to a force circle. The resultant force *R*, passes through the center of the circle, and the remaining forces can be balanced through a geometrical solution of the circle. Some of the relations developed include:

$$F_C = R\cos(\lambda - \alpha) \tag{2.3}$$

$$F_T = R\sin(\lambda - \alpha) \tag{2.4}$$

$$F = R\sin\lambda \tag{2.5}$$

$$N = R\cos(\lambda) \tag{2.6}$$

$$R = \frac{F_S}{\cos(\phi + \lambda - \alpha)} = \frac{\tau b t_1}{\sin\phi\cos(\phi + \lambda - \alpha)} \tag{2.7}$$

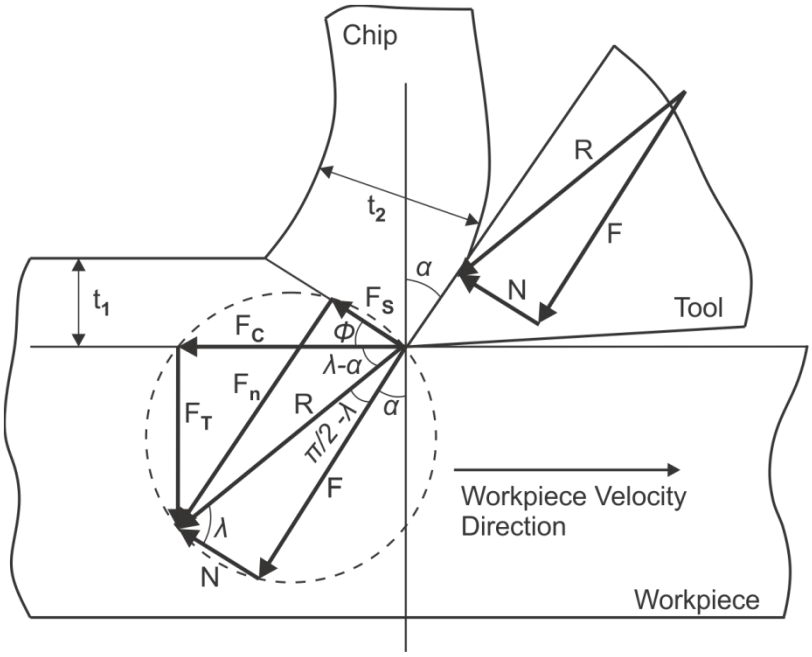

Figure 2.10 Merchant's model for orthogonal cutting [14].

From Figure 2.10, the resultant force component *R* along the shear plane can be resolved into the shear force F_s, and a normal force F_n acting perpendicular to the shear plane. For simplicity, the resultant force can be resolved into two components: the cutting force F_c, and the thrust force component F_T. Both the cutting force and thrust force can be easily measured using a tool dynamometer.

The shear angle φ can be expressed in terms of the rake angle α and the friction angle λ and can be adjusted by applying the minimum energy principle to minimize energy consumption during cutting. According the Merchant model, the shear angle can be developed as:

$$\varphi = \frac{\pi}{4} - \frac{1}{2}(\lambda - \alpha) \tag{2.8}$$

In order to decrease the forces and power consumed during cutting, the shear angle must be increased. To do so, the above expression indicates that the friction coefficient (equivalent to tan λ) between the tool and the chip must be decreased by using lubricants or materials with lower coefficients of friction. In addition, the rake angle of the cutting tool must be increased to the limit the weakened cutting edge can withstand from the pressure and friction load exerted by the chip at the rake face contact zone.

When the shear stress τ, at the shear plane and the friction angle λ, at the tool chip interface are known, plus cutting conditions and given tool geometry, according to the equations above, the orthogonal cutting forces can be predicted.

Through experiment, a parameter called the chip thickness ratio *r*, which is the ratio of undeformed chip thickness t_1 to the deformed chip thickness t_2, the shear angle can also be obtained from the following expression:

$$\tan\phi = \frac{r\cos\alpha}{1 - r\sin\alpha} \tag{2.9}$$

During machining of metals, the shear stress along the shear plane is not constant, thus there will be disagreement between the measured and theoretically calculated shear angle [13]. Merchant followed by modifying his model with the assumption that the shear stress is a function of the normal stress acting on the shear plane, which can be expressed as:

$$\tau = \tau_0 + K_1 \sigma \tag{2.10}$$

where K_1 and τ_0 are material constants, and σ is the normal stress acting on the shear plane.

Also included in Figure 2.10 above are velocity relations that are developed geometrically; they are:

$$V_C = \frac{V \sin \phi}{\cos(\phi - \alpha)} \tag{2.11}$$

$$V_S = \frac{V \cos \alpha}{\cos(\phi - \alpha)} \tag{2.12}$$

where V is the cutting velocity, V_C is the chip velocity, and V_S is the shear velocity.

2.6.2 Mechanics of Oblique Cutting

The difference in the geometry of oblique cutting may be first compared to orthogonal cutting by reviewing Figure 2.1b. From Figure 2.11, the geometrical planes indicate a plane normal to the cutting edge and parallel to the cutting

velocity V defined as the normal plane P_n. Shear deformation takes the form of plane strain without side spreading, thus the shearing and chip motion are identical on all the normal planes parallel to the cutting speed V and perpendicular to the cutting edge. Therefore, the cutting velocity (V), shear velocity (V_s), and chip velocity (V_c), are all perpendicular to the cutting edge. Similar to orthogonal cutting, the resultant cutting F, as well as other forces acting on the shear and chip-rake face contact zone, also lie on the normal plane P_n. There are no cutting forces perpendicular to the normal plane, however the cutting velocity has an oblique or inclination angle i in oblique cutting operations, and therefore the directions of the shear, friction, chip flow, and resultant cutting force vectors have components in the three Cartesian coordinates (x,y,z), as shown in Figure 2.11.

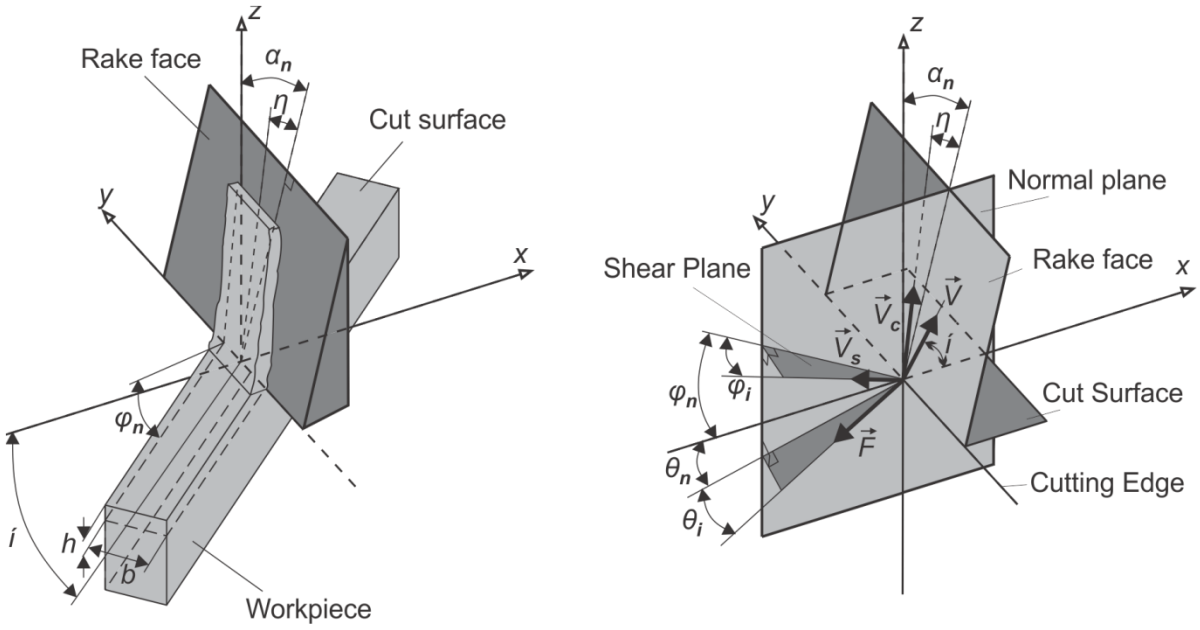

Figure 2.11 Geometry of oblique cutting [15].

The most important planes in oblique cutting are the shear plane, the rake face, the cut surface *xy*, and the normal plane P_n or *xz*. Since most analyses assume that the mechanics of oblique cutting in the normal plane are equivalent to that of orthogonal cutting, all velocity and force vectors are projected on the normal plane. As shown in Figure 2.12 below, the angle between the shear and the *xy* planes is called the normal shear angle φ_n.

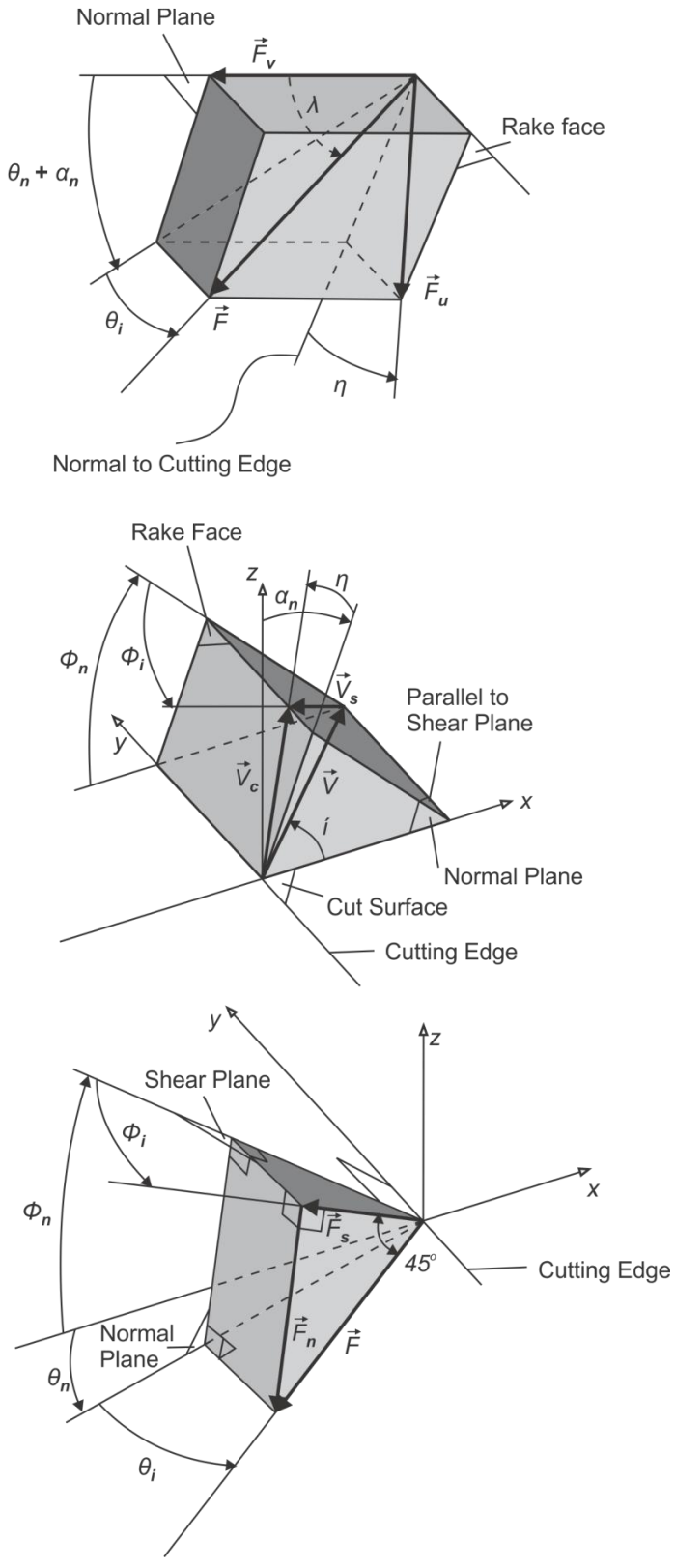

Figure 2.12 Force, velocity, and shear diagrams in oblique cutting [15].

On the shear plane lies the shear velocity which makes an oblique angle Φ_i, with the vector normal to the cutting edge on the normal plane. The shearing chip flow moves along the rake face plane with a chip flow angle η measured from a vector on the rake face but normal to the cutting edge and also lying on the normal plane. The frictional force between the chip and the rake face is collinear with the direction of chip flow. The angle formed between the *z*-axis and the rake face is defined as the normal rake angle α_n. The friction force F_u along the rake face and the normal force to the rake F_v form the resultant cutting force *F* at a friction angle β_a, as shown in Figure 2.12 above. The resultant force *F* projects an acute angle of θ_i with the normal plane, which in turn has an in-plane angle of (θ_n + α_n) with the normal force F_v. The angle θ_n is the angle between the *x*-axis and the projection of *F* on the normal plane. From Figure 2.12, the following geometric relations can be derived:

$$F_u = F\sin\beta_a = F\frac{\sin\theta_i}{\sin\eta} \rightarrow \sin\theta_i = \sin\beta_a\sin\eta \tag{2.13}$$

$$F_u = F_v\tan\beta_a = F_v\frac{\tan(\theta_n+\alpha_n)}{\cos\eta} \rightarrow \tan(\theta_n+\alpha_n) = \tan\beta_a\cos\eta \tag{2.14}$$

The chip velocity $\overrightarrow{V_C}$, shear velocity $\overrightarrow{V_s}$, and cutting velocity $\vec{V}$, can each be defined by their corresponding Cartesian components:

$$\vec{V} = (V\cos i\,,\ V\sin i\,,\ 0) \tag{2.15}$$

$$\overrightarrow{V_C} = (V_C\cos\eta\sin\alpha_n\,,\ V_C\sin\eta\,,\ V_C\cos\eta\cos\alpha_n) \tag{2.16}$$

$$\overrightarrow{V_s} = (-V_s \cos\phi_i \cos\phi_n\,,\ -V_s \sin\phi_i\,,\ V_s \cos\phi_i \sin\phi_n) \tag{2.17}$$

Through elimination of *V, V_C, and V_s* from the velocity relations

$$\vec{V_s} = \vec{V_C} - \vec{V}$$

the geometric relation between the shear and the chip flow directions can be derived:

$$\tan\eta = \frac{\tan i \cos(\phi_n - \alpha_n) - \cos\alpha_n \tan\phi_i}{\sin\phi_n} \tag{2.18}$$

The relationships generated above are used to define the geometry of the oblique cutting process.

2.7 Chip Formation

During a machining process, a large stress generation occurs as the tool penetrates the workpiece. Initially, elastic deformation occurs as the stress reaches the yield stress of the work material, then plastic deformation starts and is followed by the formation of a chip. The boundary line between the chip and workpiece, or the line separating the deformed from the undeformed material, is the shear plane. The angle between the shear plane and cutting speed direction is the shear angle. In hard turning, chip segmentation starts when the material in front of the tool is compressed, and the compressive stress initiates a crack on the free surface. As the tool advances (Figure 2.13), the initiated crack propagates towards the cutting edge, and it stops before reaching the tool tip [16]. A saw-toothed chip is a typical feature of hard turning, and this type of chip is defined as a continuous chip with variation in thickness.

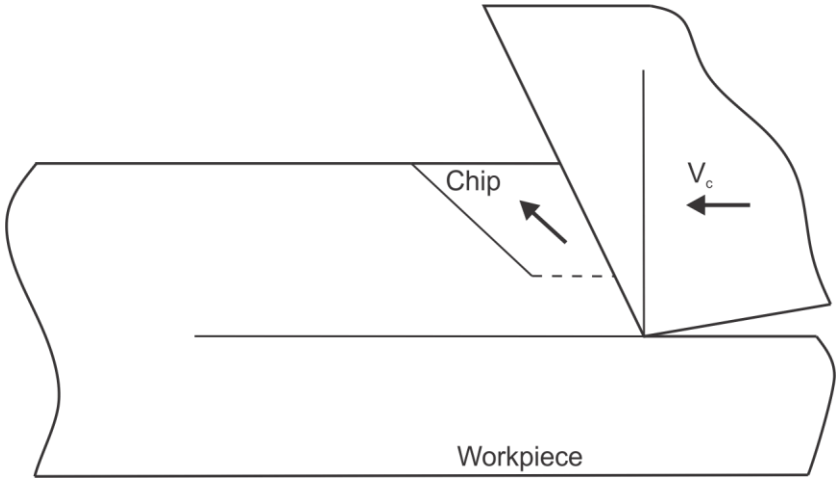

Figure 2.13 Chip formation mechanism [16].

2.8 Surface Quality

Generation of a new surface is one of the main purposes of machining and the quality produced affects the performance of the machined part. The types of chips formed, the tool profile, and the process parameters will determine the surface finish during metal cutting. Continuous and discontinuous chips will generate different surface finishes. Generally speaking, a continuous chip with no built-up-edge (BUE) generated is more desirable as it keeps the cutting force fluctuations minimized and the cutting conditions stable. At a minimum, if these conditions are met, the tool profile will be reproduced on the workpiece surface and this pattern is referred to as 'feed marks'. By standard methods, the surface finish can be specified, and it is called surface roughness, measured in micrometers (μm).

Nakayama et al. [17] studied the surface quality after hard turning with single a point tool. It was demonstrated that flank wear does not affect the surface finish until the cutting edge becomes rough and deteriorates the surface. Chen et al. [18] showed the influence of rake angle, inclination angle, cutting speed, and feed rate on the surface waviness and roughness. Penalva et al. [19] concluded that rubbing from flank wear cannot influence the quality of the machined surface much, since the cutting edge shifts due to tool wear, keeping the contact area between the flank and workpiece small.

2.9 Rotary Tools

For most practical machining operations, the same portion of the cutting edge and rake face of the cutting insert are continuously in contact with the moving chip, which generates high tool-chip interface stresses and temperatures, tool wear, and eventually tool failure. However, as a benefit, the moving chip flow transfers a large percentage of the total heat generated during machining away from the tool-chip interface. Without this heat transfer, much higher temperatures and lower tool life are expected, possibly threatening the economical viability of machining operations. Thus, a method to decrease the tool wear rate is to continuously change the portion of the cutting insert in contact with the workpiece during a machining operation. A tool with infinite cutting edge length would thus be required to satisfy this criteria. However, a more practical alternative includes the use of a circular shaped cutting insert which has the

ability to rotate about its axis such that the engaged cutting edge is continuously fed into the tool chip interface zone. This would generate cyclical exposure of the cutting edge and rake face to the chip formation process. The cyclical behavior allows for a ‘rest’ period between engagements and such a process is often coined as the ‘self-cooling’ feature of the tool. Such tools are referred to as ‘rotary tools’ and the machining process associated with these tools may be called the ‘Rotary Tool Cutting Process’.

The geometry of the rotary cutting tool is a frustum of a cone which can be orientated such that the base acts as the rake face (Type I) or with the cutting tool positioned vertically and the cone peripheral surface acting as the rake face (Type II), as shown in Figure 2.14 below.

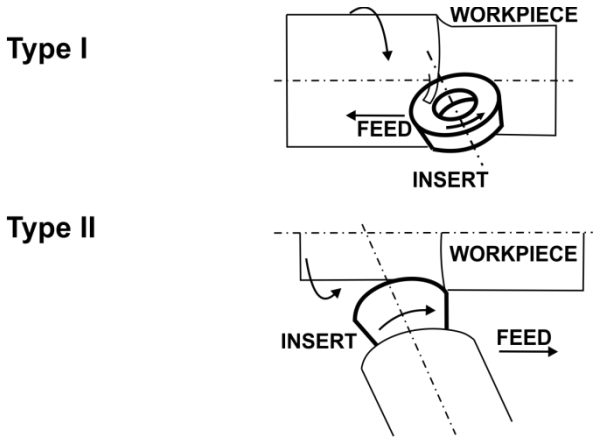

Figure 2.14 Rotary tool types in different orientations [20].

The cutting tool, known as an insert, rotates simultaneously with the workpiece in addition to its linear feed motion. The spinning action of the insert supplies the fresh cutting edge to the workpiece being machined. The cooling time for an individual cutting point on the insert is much higher than the cutting time for the same point [20].

Very fine machined surfaces can be obtained with the rotary tool, provided the tool spindle assembly is adequately rigid, due to the circular profile of the cutting insert. Rotary tools are also classified into two different categories: driven or self-propelled. For the self-propelled rotary tool (SPRT), the insert is rotated by the cutting force and chip flow on the rake face, whereas a driven rotary tool (DRT) is rotated by an independent external power source, such as a motor. It is essential in SPRTs that an inclination angle exists between the insert's spinning axis and the cutting velocity. This ensures that the tool will be propelled in the appropriate direction during the chip formation process. If the case is the opposite and the insert's spinning axis is set parallel to the workpiece cutting velocity (i.e. the workpiece velocity is perpendicular to the cutting edge and therefore cutting orthogonally), then the tool cannot be propelled by the chip flow.

Table 2.2 below lists the historical development of rotary tools. This clearly illustrates that the fundamental principle of rotary tools dates back to the 19th century by James Napier [1], however, little information on this machining process existed prior to the 1930's. It is reasonable to assume that the reasons for rotary tools not becoming commercially available is largely due to the difficulty in ensuring consistent performance and possibly the inability of rotary tools to

accept other insert shapes besides disc-like inserts. Currently, improvements on structural design and industrial applications of rotary tools have been of particular interest.

Table 2.2 Development of Rotary Tools [1].

1868	James Napier foresaw the great advantage and important commercial possibilities of rotary cutting tools
1930s	First publications of rotary cutting tools appear
1950s	Intensive studies begin. Shaw and co-workers develop driven rotary cutting tool and explore the kinematics of rotary cutting. Findings are summarized and cover the influences of the motion of the cutting edge, workpiece and chip formation, cutting forces, and cutting temperatures. Shaw's work formed the basis for research in this area of machining.
1960s and 1970s	Research peaked in the Soviet Union with the development of Type II rotary tool.

After James Napier's epiphany, Shaw et al. [1] presented an analysis of a driven rotary tool cutting a steel tube's end. In this study, the curvature of the cutting edge of the round disc insert was assumed to be straight considering that the diameter of the insert was much larger than the depth of cut in practice. The rotary tool machining operations were compared with the conventional orthogonal and oblique cutting cases. Considering that the cutting tool insert was spinning, absolute chip-flow and relative chip-flow velocity concepts were produced as well as absolute chip-flow and relative chip-flow directions. Fundamental velocity and force relations were also presented in this study.

Between 1962 and 1972, there were research advancements on the practical applications of rotary tools with the objective of developing cutting models and assessing the claimed merits of rotary tools. Zemlyanskii et al. [21-30] investigated a series of turning operations with a 'Type I' self-propelled rotary tool. They used a high speed steel (HSS) rotary tool on a large range of workpiece materials including copper, pure zinc, carbon steel, brass, nickel based alloys, titanium alloys, and cast iron with a wide range of cutting conditions. Through the study, they showed the cutting force and thrust forces were affected by the rotary tool axis inclination angle, while the feed force remained practically unchanged. This series of work also demonstrated the effect of cutting speed and the workpiece material on the cutting forces. Different rake angles from -5^{o} to 20^{o} were examined and slight drops in forces were observed in higher positive rake angles. Furthermore, the increase in depth of cut of the rotary tool insert diameter results in a higher cutting force and thrust

force. Granin [31, 32] also used a 'Type I' self-propelled rotary tool experiment setup for the study of rotary machining surface finish and tool life. In this study he developed a theoretical surface finish equation and proved that the type I self-propelled rotary tool was capable of generating very fine surface quality compared to the surface obtained by a conventional stationary tool insert at the same feed rate. Tool life was also shown to be 4000 times that of the conventional stationary tool. The prolonged tool life was due to the lower coefficient of friction on the rake face, lower temperatures in the cutting zone, and significant increase in the active length of the cutting edge in the rotary cutting process. Reznikov and Koosher [33-37] studied 'Type I' self-propelled rotary tool kinematics. This work demonstrated that every point on the rotary tool cutting edge remains in contact with the workpiece for a very short period (approximately 0.2-0.3 seconds), therefore the temperature in a rotary tool was shown to be 40% lower than the temperature during the conventional stationary cutting process. They also applied the developed fixtures for the self-propelled rotary tool in the turning and shaping process. Konovalov and Tarakanov [38, 39] studied 'Type II' self-propelled rotary tools in machining of plane surfaces. These types of rotary tools were mainly used in finishing or semi-finishing processes. Through this work they were able to develop theoretical roughness expressions for 'Type II' rotary tools. Venkatesh et al. [40] have used HSS self-propelled rotary inserts for face milling on mild steel and made comparisons with the stationary inserts used in the same machining process with identical cutting conditions. Comparable surface finishing values were observed. Also, they

demonstrated no built-up-edge formation in the rotary tool machining and the high tool wear resistance of this type of tool. Lower cutting temperatures were also verified by the comparison of the generated chip color with the stationary tool machining.

With the increasing demands of high performance materials in the aerospace and automobile industries, the challenges in machining such materials also rise. Such materials include metal-matrix composites (MMC), titanium, and nickel based Waspaloy. P. Chen [41] carried out a study on the machining of MMC (SiCw/Al) with self-propelled rotary tools. The performance of the self-propelled rotary tool was collected. Carbide tool life can be extended remarkably by using rotary tools (approximately 50 times compared to the fixed circular insert cutting and 112 times compared to a square-profiled insert). The rotary tool is capable of high-speed cutting and high-feed rate cutting. The improvement of the rotary tool performance was attributed to the even distribution of tool wear along the entire circumference of the insert cutting edge, reduction of the effective cutting speed due to the rotation of the insert, and the decrease of cutting forces. An experimental investigation was also performed by Kishawy et al. [42] to evaluate the performance of self-propelled rotary tools in high-speed dry face milling of cast iron. The wear resistance of the rotary tool was found to be superior compared to the single point cutting tools. A model was also developed by Kishawy et al. [43] to analyze the characteristics of heat transfer and temperature during rotary tool machining. It was noted that the optimized driven rotary tool insert rotating speed could minimize the cutting temperature. In 2004, Vincent

Dessoly et al. [44] generated a tool temperature distribution model for self-propelled rotary tool machining of hardened steels. They utilized the moving heat source theory and generated a finite element model (FEA) to obtain the solution. Good agreement was found with the predicted and experimental results gathered from an infrared camera. Cutting temperatures for self-propelled rotary tool machining were found to be lower (by approximately 50°C) compared to that obtained with a conventional non-rotating circular fixed tool under identical cutting conditions. In 2003, hard turning using self-propelled rotary tools on heat-treated steel was studied by Zhang [45], which outlines a new method for the finishing process with no coolant, high material removal rate and superior tool life. Shuting Lei et al. [46] developed a new generation of driven rotary tools for high speed machining of titanium (Ti-6Al-4V). The cutting forces were not sensitive to the change of cutting speeds in the range between 240 and 480 m/min when using driven rotary cutting tools. Tool wear leading to short insert life in driven rotary tools during high speed machining is generated by the thermal interactions. They also mentioned that the increased tool life of rotating tools also improves productivity by reducing indexing time. Armerago et al. [47-49] came up with predictive models for the fundamental rotary tool cutting process. They developed an equivalent oblique cutting model for the rotary cutting process, including the consideration of insert rotating velocity. Leiming Li [50] generated a force model for the self-propelled rotary tool cutting process based on the equivalent transformation method, circular shape (nose radius) cutting edge chip flow prediction method and orthogonal cutting force prediction

method. This work also presented relative chip flow direction prediction and absolute chip flow direction which resulted in good agreement with experimental results (average error percentage was lower that 10%). It was also concluded that increasing the feed or cutting velocity would result in a lower friction coefficient when the other cutting conditions remained unchanged.

In summary, the primary benefits of rotary cutting tools include:

1. Several hundred-folds increase in tool life, considerably higher than those for any other tool of the same material.
2. Reduced cutting temperatures.
3. Improved machining of difficult-to-cut materials like titanium and nickel based alloys.
4. Higher material removal rates during machining.
5. Very fine machined surface (provided tool spindle assembly has adequate rigidity).

The following may hinder the application of rotary tools in the manufacturing industry:

1. No matter how precise (or accurate) the rotating parts have been produced, a cutting edge in motion may always generate more errors than a stationary one.

2. Severe chatter may occur due to the large tool radius and poor stiffness of the rotary system.
3. Stepped workpieces cannot be produced with rotary tools.

2.10 Principles of Rotary Cutting

Rotary cutting principles differ from conventional cutting theories due to its unique kinematics character. Important considerations in rotary cutting are inclination angle of the cutting edge, chip flow angle and rake angle, cutting speed, chip deformation, and tool wear.

The inclination angle (*i*) is the most important factor affecting the performance of rotary cutting. Since the circular inserts have an arc-shaped cutting edge, the tangent at different points is at different angles to the tool reference plane (i.e. the edge inclination along the arc varies) [51]. The circular cutting edge angle also varies with change in inclination angle. The tool nose here refers to the point where the cutting edge is zero, as shown in Figure 2.15 and Figure 2.16 below.

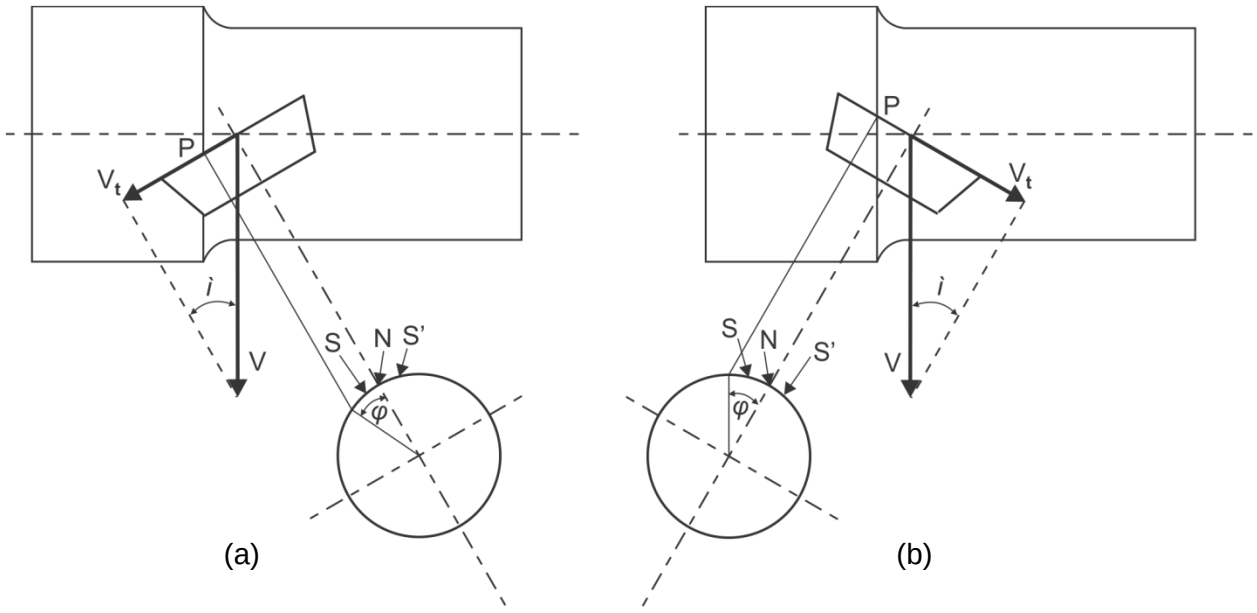

Figure 2.15 Type I rotary cutting tools with (a) positive inclination angle and (b) negative inclination angle [51].

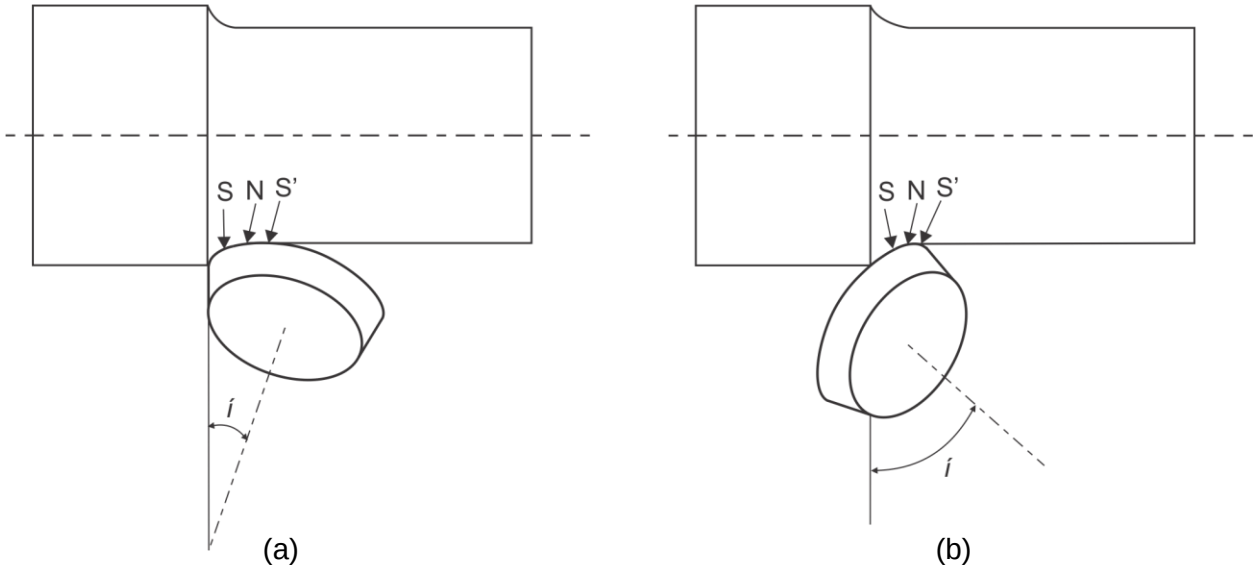

Figure 2.16 Type II rotary cutting tools with (a) positive inclination angle and (b) negative inclination angle [51].

The orientation of the inclination angle is also expressed differently. Normal/reverse cutting or normal/reverse feed are common expressions used based on the direction of chip flow, tool rotation or feed motion. The tool nose separates the cutting edge into two parts: major cutting edge (*S* in Figure 2.15 and Figure 2.16) on the side towards the feed direction, and minor cutting edge (*S'* in Figure 2.15 and Figure 2.16) on the other side. When the tool nose is the highest point on the major cutting edge, the edge inclination is said to be positive (Figure 2.15(a) and Figure 2.16(a)), otherwise it is negative (Figure 2.15(b) and Figure 2.16(b)). This definition is in agreement with BSI296: Part 2, 1972 [52]. An increase in bearing friction decreases the equivalent inclination (*i*) of a SPRT. This raises the relative workpiece cutting speed (V_{wr}) and the relative chip flow

velocity (V_{cr}) and hence the cutting temperature and energy consumption. These will in turn accelerate tool wear.

The cutting speed refers to the peripheral velocity of the workpiece following the convention in ordinary metal cutting and independent of the rotary motion and tool geometry. The relative workpiece cutting speed is closely related to the tool edge inclination and rotation of the tool and is actually the cutting speed of an equivalent oblique or orthogonal tool; for a driven or self-propelled rotary tool respectively [53]. These velocity relations for self-propelled rotary tools are illustrated below.

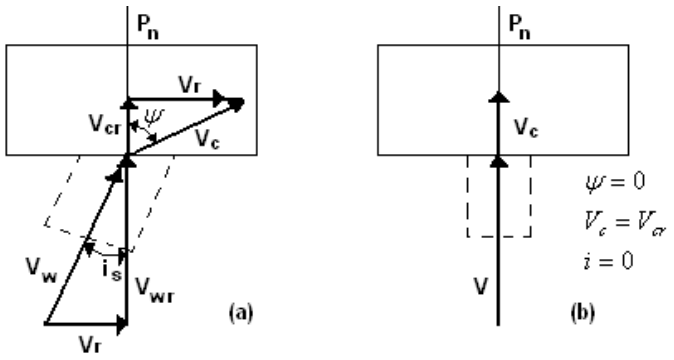

Figure 2.17 Simulated self-propelled rotary cutting (a), and equivalent orthogonal cutting model (b) [53].

Referring to Figure 2.17, for a SPRT with static inclination angle 'i_s' not equal to zero and the tool is free to rotate, then the initial cutting action will distribute a cutting force along the cutting edge which supplies the propelling motion to the insert. The forces acting along the cutting edge will accelerate the

tool insert until equilibrium is reached when no additional side force acts along the tool cutting edge and provides no resistance. This is possible if assuming free rotation and friction and chip transportation requires no additional energy. This particular instance will occur when the resultant relative workpiece velocity V_{wr} is normal to the cutting edge and the angle of inclination i (defined by the angle made with V_{wr} vector and the normal to the cutting edge at undeformed chip width center), is zero.

From the figure above, the velocity relations become:

$$V_{wr} = V_w \cos i_s \tag{2.19}$$

$$V_r = V_w \sin i_s \tag{2.20}$$

So to initiate the self-propelling motion of a freely rotating insert, a static inclination angle must exist as it ensures the generation of the force along the cutting edge which accelerates the insert until equilibrium at a tangential velocity V_r.

2.11 Factors Affecting Rotary Tool Life

During a machining process, the rotation of a self-propelled tool is generated 'naturally'. This results in low sliding speed, pressure, and temperature at the tool-chip interface. Due to continuous motion of the cutting edge of rotary tools during machining, a long non-working period for any point (*p*)

on the cutting edge makes the practical cutting path of the point to be reduced by *k* times. The life of the rotary tool is therefore *k* times as long as that of a conventional round stationary tool, if other factors are not considered.

2.11.1 Tool Geometry

Increase in the edge inclination angle (*i)* reduces the relative cutting speed (V_r), relative chip flow velocity (V_{cr}), power consumption, cutting temperature, the degree of chip formation and the unit cutting forces. These factors result in a decrease in tool wear intensity. The edge inclination angle has a significant effect on the life of rotary (from a tool design standpoint), and only a little effect on the fixed circular inserts. For example, increasing the inclination angle from 15^o to 30^o gave a 72% increase in tool life at high cutting speed (240m/min) and a further tilting to 45^o increased tool life by 145% due to lower relative cutting speed [18]. The percentage improvement in tool life (Kr) due to variation of edge inclination can be estimated by:

$$Kr = \frac{V}{Vr} = \frac{1}{\cos i} \tag{2.21}$$

However, an increase in inclination angle may also cause variation of the effective working angles along the curved cutting edge, an increase in the rotary speed of the self-propelled tool and hence aggravate fatigue problems. The resulting influence of the edge inclination on tool wear comes from these two opposing effects.

The diameter of the insert used has more influences on the rotary tool wear. Foremost, wear of a rotary tool spreads around its circumferential cutting edge. Thus a larger insert will have a longer cutting edge and thus reduced tool wear. Second, an increase in the radius of the tool will decrease the tool contact angle subtended by the tool-workpiece contact arc, thereby reducing the variation of the working angles along the arc. This slows down the rotational speed, lowers the fluctuation of strain and stress, and reduces the tendency for fatigue wear [51]. Third, a large insert may induce vibration easily, causing chipping of the cutting edge. Fourth, the rake and clearance angles ground on the insert influence the working angle, the heat capacity of the cutting edge, and the friction between the flank face and the machined surface; all of which affect SPRT tool life.

2.11.2 Bearing System

As mentioned earlier, an increase in bearing friction decreases the equivalent inclination (i) of a SPRT. This raises the relative workpiece cutting speed (V_{wr}) and the relative chip flow velocity (V_{cr}) and hence the cutting temperature and energy consumption. These effects will accelerate tool wear.

2.11.3 Tool Wear Mechanisms

Chip and flank wear are the predominant failure modes when machining with self-propelled rotary tools [51, 18]. Abrasion wear mechanisms are common

with SPRTs during high speed cutting conditions since the softened chip particles tend to stick to the rotating tool surface, which then cycles through the tool-chip interface. Using self-propelled rotary tools also produces stable built-up-edges (BUE) at higher cutting speeds due to decrease in cutting temperatures, which results in a wider cutting range where BUE would normally occur.

Oxidation often occurs on the cutting edge of rotary tools more often than stationary tools because of the shorter cutting time and longer exposure to air the cutting edge experiences. This generates oxide films that can prevent adhesion of work materials to the rotary tool, as well as diffusion wear of the tool (a wear mechanism already reduced by rotating tools because of the lower cutting temperatures). Fatigue wear is more likely in rotary tools (as the tool edge undergoes regular intervals of fluctuating temperatures), especially when machining with carbide inserts. This can be illustrated by thermal cracking of rotary tools along the radial direction of a circular carbide insert with prolonged machining [51, 18]. The number and length of cracks increase almost linearly with cutting time. At a certain point, networks of cracks are formed, resulting in breakage of grain structures or aggregates of the tool particles and eventual fracture of the cutting edge.

2.12 Rotary Tool Application

For proper operation, an SPRT must have a minimum value of edge inclination angle (*i*) in order to provide the necessary driving forces to rotate the

insert. Keeping in mind the forces necessary to overcome bearing friction, minimum values of edge inclination angles include 2.50-7.50^{o} [54] and a maximum of about 72^{o} [51].

Cutting speed employed in SPRT is determined by the tool material, workpiece material, and the expected tool life. Feed rates tend to be cutting condition and dynamic response dependant. For example, a very low feed rate may excite chatter and deteriorate the machined surface in practice. In this case, improved surface finish can be obtained by increasing the feed rate until the surface profile is characterized by feed lines [55, 56]. Since rotary tool inserts are circular, the tool-workpiece contact is long and results in larger cutting forces and chatter when compared to conventional profiled inserts (i.e. square, rhomboid, etc.). The depth of cut has a large influence on the length of the contact arc. The power consumption and rigidity of the entire machining system are the primary factors when determining depth of cut.

Cutting temperature, as discussed earlier, has a significant effect on finish quality and on tool life when machining with SPRT. Cutting speed and inclination angle of the insert affect the cutting temperature. When the inclination angle is increased, cutting temperature decreases due to the reduced amount of work required for workpiece material deformation and friction on the rake face of the tool. An improvement in heat transfer from the cutting zone is also achieved due to the increase in insert rotational speed. Increase in workpiece cutting speed leads to increased cutting temperatures, similar to conventional machining, and an increase in depth of cut and feed rate have the same effect. Self-propelled

rotary tools tend to generate cutting temperatures on the range of 50-150^{o}C lower than fixed circular tools [55].

2.13 Surface Integrity and Quality

Increasing feed generates a better surface quality when using a SPRT. Better surface finish occurs at inclination angles lower than 10^{o} [55]. Cutting speed has negligible effect on the surface finish generated in rotary tool machining. Compressive residual stresses and thus higher surface strength and fatigue life are normally generated with rotary tool machining unlike conventional machining which produces tensile residual stresses. The magnitude of the compressive residual stress increases with an increase in inclination and bearing friction. Thermal damage on the machined surface is also reduced given the lower cutting temperatures of rotary tool machining.

2.14 Structure and Design of Self-Propelled Rotary Tool

Very fundamental factors must be considered during the design of a self-propelled rotary tool:

1. Tool structure, including fixture and base of insert, must be very simplistic.
2. Tool structure should be durable, accurate and easy to maintain.

3. The tool structure should be easily assembled and coupled to a standard lathe tool post or turret.

Tool geometry should allow the largest possible depths of cut, feed rate, stable cutting, superior surface finish, low relative cutting speed (V_r) and low cutting temperature. Very large nose radius inserts, excessive running clearance of the bearing and eccentricity of the circular cutting edge could cause chatter during machining. A simple solution here would be using a much smaller radius insert, high inclination angle, and reduced eccentricity of the insert.

CHAPTER 3

EXPERIMENTAL SETUP

The factors outlined in Section 3.6 were considered in the development of a prototype self-propelled rotary tool for hard turning, capable of accepting inserts with ISO designation RCMT 09 T3 00 (Appendix A). The largest focus of the design was the bearing system such that it would withstand high running speeds and high radial and thrust loads with relatively low friction and minimum eccentricity under dynamic conditions. A structure with two needle roller thrust bearings and one radial needle roller bearing was designed to achieve a lower coefficient of friction and reduced cost. A detailed explanation of the tool designed is outlined in Appendix B.

3.1 Cutting Tool Configuration

Dry hard turning tests were conducted to examine the performance of the prototyped self-propelled rotary tool. The tool is configured such that the insert's cutting edge is positioned with a fixed inclination angle i = 25º and a normal rake angle α_n = -5º. The insert and cutting tool used are shown in Figure 3.1 below.

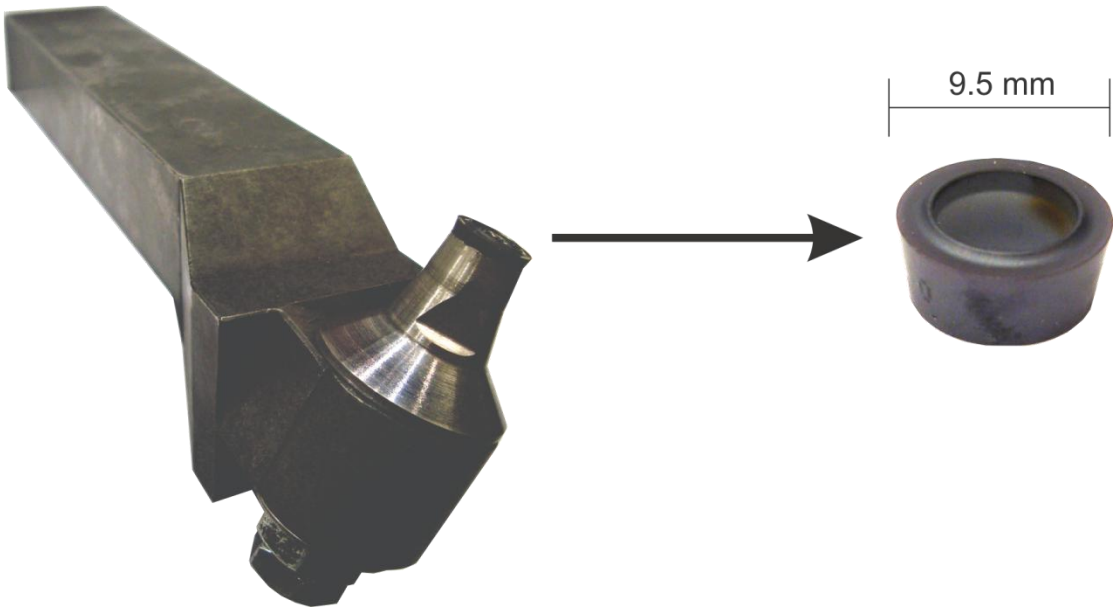

Figure 3.1 Prototype self-propelled rotary tool for hard turning (left) which uses standard ISO insert (right).

The inserts used were uncoated carbide and had a diameter of 9.5mm and clearance angle of 7º. These inserts are readily available and manufactured by many machining companies in different grades and/or with different coatings. The inserts used during the experiment were graciously donated by Kennametal ®.

For fixed cutting conditions, the thrust bearings were removed from the tool holder assembly, replaced with washers, and clamped securely to deny insert rotation.

3.2 Workpiece Materials

The materials used in this experiment were AISI 4140 steel and Grade 5 Titanium (Ti-6Al-4V). The 4140 steel was heat-treated to obtain a 'hard-to-cut' material status (i.e. 54-56 HRC). The compositions of the steel and titanium samples are listed in Table 3.1 and Table 3.2, respectively.

Table 3.1: Composition of AISI 4140 Steel.

Component	Content %
C	0.38 – 0.43
Mn	0.75 – 1.00
P	0.035 Max
S	0.04 Max
Si	0.15-0.30
Cr	0.80 – 1.10
Mo	0.15 – 0.25

Table 3.2: Composition of Titanium (Grade 5, Ti-6Al-4V).

Component	Content %
Al	5.5 – 6.75
Fe	0.25 Max
O	0.20 Max
Ti	Balance
V	3.5 – 4.5

The materials used had standard stock size diameters of 25.4 mm, and were cut to lengths of 304.8 mm.

3.3 Auxiliary Equipment

During each cutting pass, the insert rotation speed was measured and recorded using a laser tachometer (E655Digital©, +/- 0.05% accuracy). The bottom side of the rotating insert holder was used as a reference for measurement, which required special placement of a small reflective strip and colouring the remainder of the surfaces black. This allowed for the tachometer to read the reflection of an emitted laser beam off the reflective strip and thus measure tool/insert speed (RPM). After each pass, the surface roughness was measured using a surface roughness tester (Mitutoyo© SJ-201), and samples of chips were collected for observation. Following each pass (SPRT tests), the tool flank wear was also measured at several locations about the circumference. The measurements were obtained through the use of a tool maker's microscope (Mitutoyo©) and were averaged and recorded. Similarly, for fixed tool cutting, flank wear was measured at the arc segment used in cutting and the maximum value was recorded.

A digital camera was also used to record video clips during the cutting process. The camera was fixed to view the tool chip zone, workpiece, and feed motion of the tool. Figure 3.2 and Figure 3.3 show an equipment setup schematic and picture, respectively. A Leadwell® T-6 turret-type CNC lathe was used for the cutting tests.

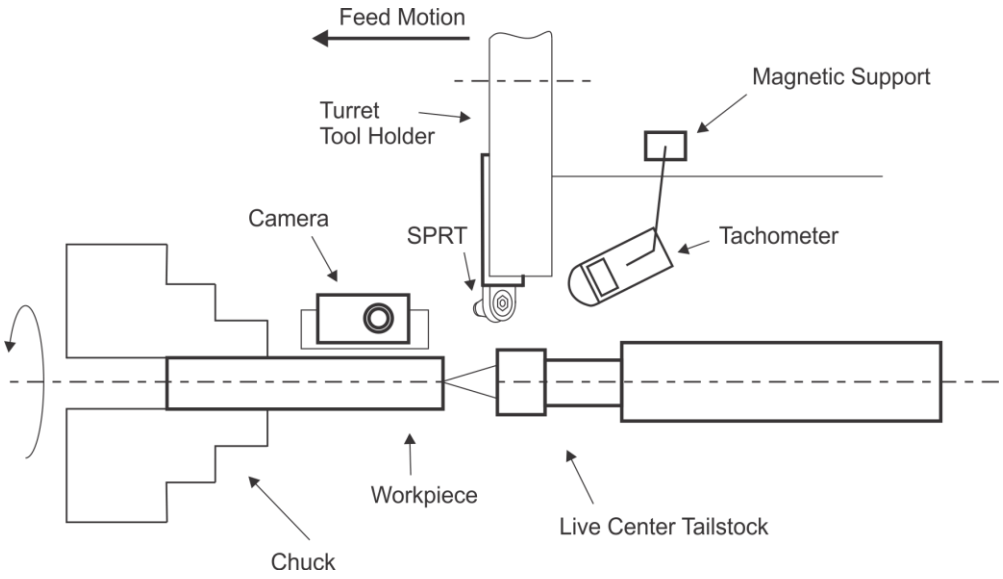

Figure 3.2 Schematic of setup.

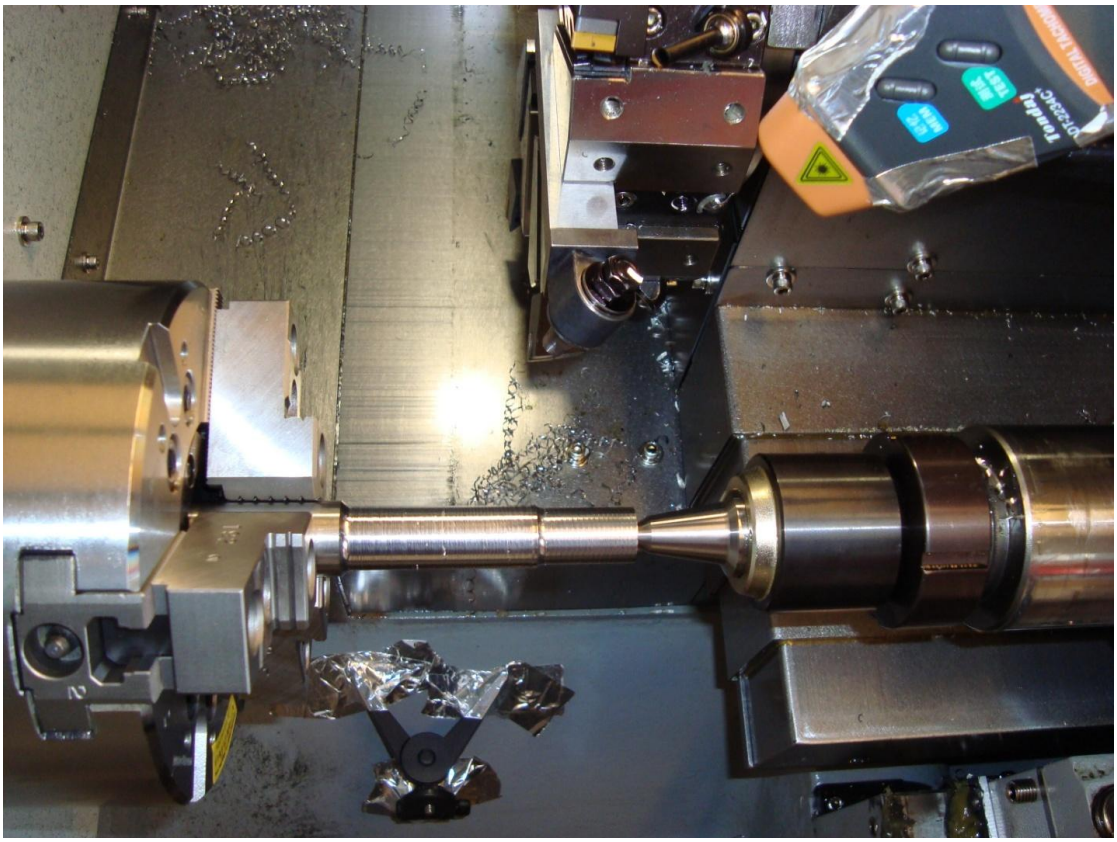

Figure 3.3 Machine and tool setup.

3.4 Cutting Conditions

In this experiment, each workpiece was machined with different cutting speeds; 4140 steel was machined using a cutting speed of 280m/min, and titanium was machined using a cutting speed of 200m/min. Depths of cut for steel and titanium were 0.3mm and 0.2mm respectively. The feeds for both materials were 0.150mm/rev, 0.225mm/rev, and 0.300mm/rev. The machining was dry cutting; no coolant was used.

3.5 Summary

The experimental data presented in the following section includes: insert rotation speeds, surface roughness, chip formation, and flank wear. The insert rotational speeds account for the relative relations in the rotary cutting process.

Several comparisons are made between the collected data and cutting condition parameters and are shown in Chapter 5.

CHAPTER 4

RESULTS AND DISCUSSION

For both material workpieces, all conditions for cutting were executed and successfully completed. As seen from Figure 4.1 and Figure 4.2, it is clear the developed prototype tool achieves the tool life benefits of self-propelled rotary tools. Given a limitation in material supply, the prototype tool was able to prolong insert tool life by a minimum of 55 times to that of the fixed tool when cutting AISI 4140 Steel, and a minimum tool life improvement of 4 times to that of fixed tool when cutting Grade 5 Titanium. It should be noted here that the carbide inserts used were employed for all tests, and are not designed for machining of Titanium materials; proving another benefit of the SPRT. As discussed earlier, flank wear *VB*, is often used to gauge tool life. Generally, if the flank is evenly worn, tool wear of 0.3mm is the maximum allowance. Beyond this point, the tool cannot be used for finishing operations. In addition, if a catastrophic failure occurs, the tool is no longer capable of cutting. Through all the tests conducted in this thesis study, these two aforementioned criteria are followed.

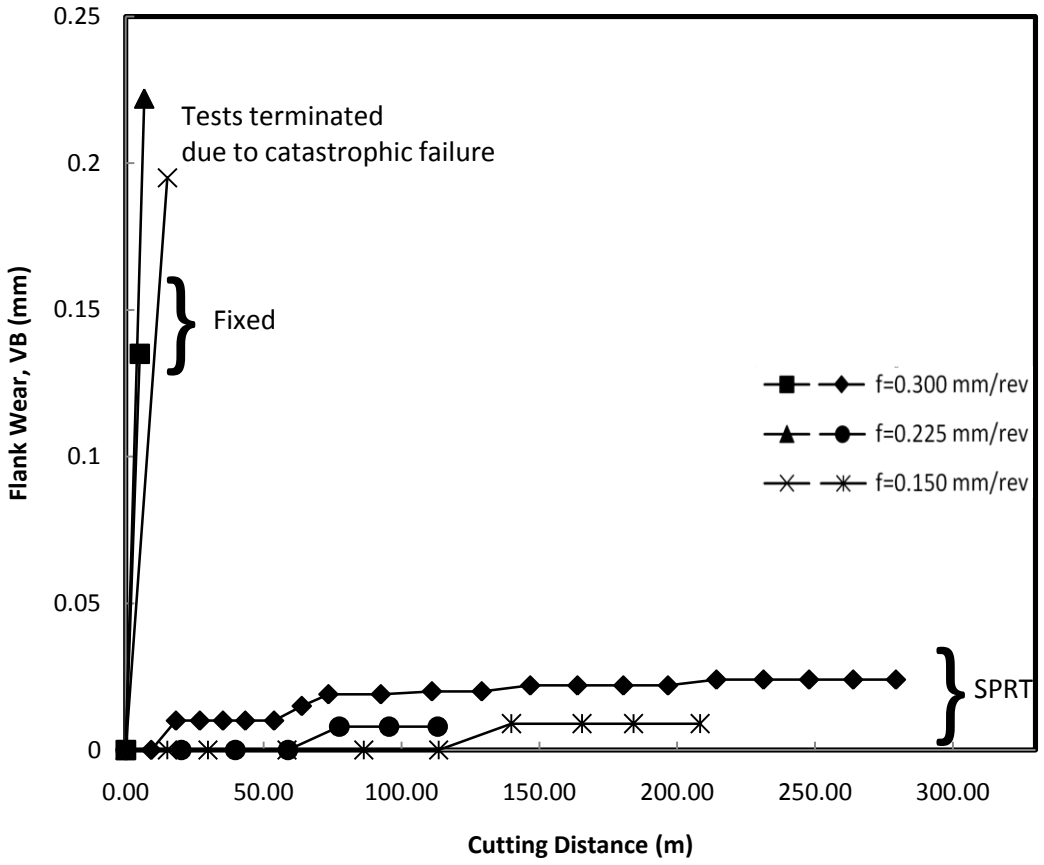

Figure 4.1 Progression of tool wear during the machining of AISI 4140 (V_w = 280m/min, d = 0.3mm, 9.5mm carbide insert).

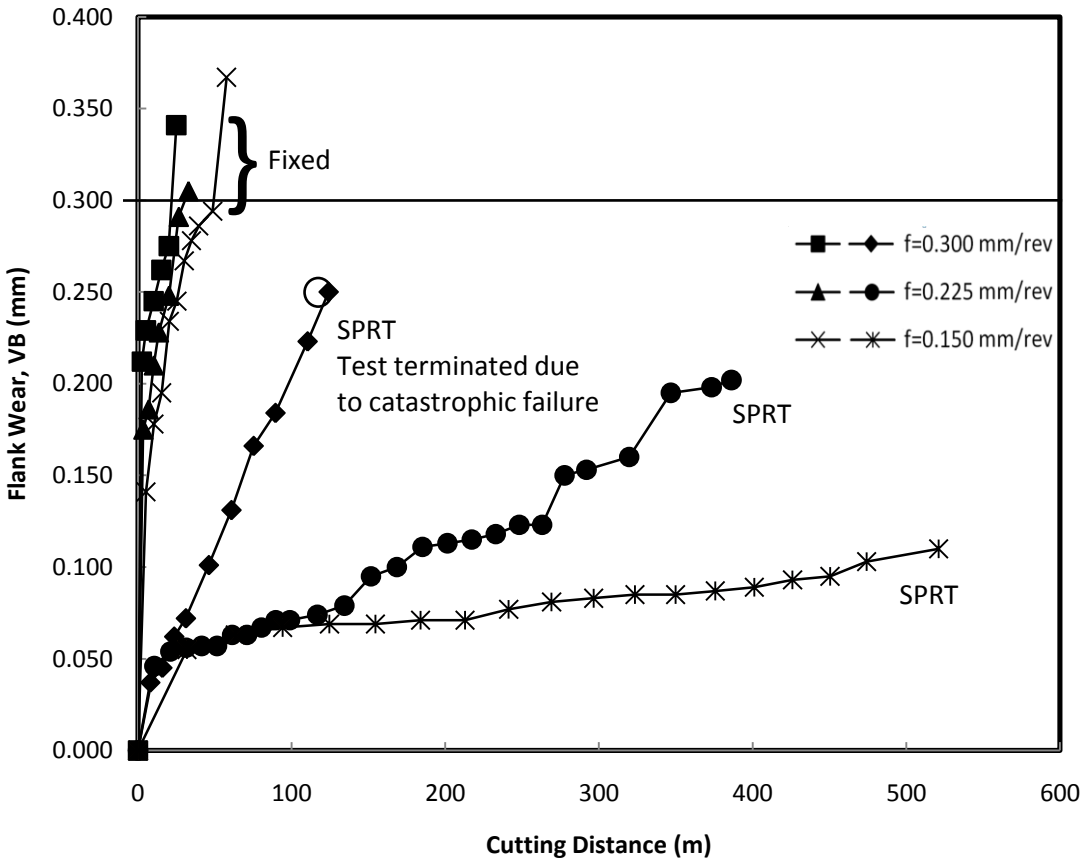

Figure 4.2 Progression of tool wear during the machining of Grade 5 Titanium (V_w = 200m/min, d = 0.2mm, 9.5mm carbide insert).

4.1 Characteristics of Tool Wear

The carbide inserts showed different wear characteristics in their fixed and rotating cutting conditions. Brand new, the inserts appeared shiny on both their flank and rake faces. For fixed inserts, the machining tests of AISI 4140 steel produced catastrophic failure of the insert's cutting edge. Preceding tool failure, the dominant wear mechanism was developed on the rake face and right before catastrophic failure, crater wear was clearly visible. For self-propelled rotary tool cutting, the carbide inserts carried uniform wear on both the flank and rake face during cutting of AISI 4140 steel. Under high feed rate (0.3mm/rev), local failures were developed on the cutting edge (chipping), but were not significant enough to jeopardize tool life or machining quality and performance.

For fixed inserts during machining of Grade 5 titanium, very aggressive and rapid flank wear was observed. As mentioned earlier, the grade of carbide inserts used were not designed for the machining of titanium materials and thus the observations reported here should not represent common wear characteristics for the fixed cutting tool conditions. However, these tests can be used to simulate machining under more aggressive conditions (such as increased material removal rate) and can predict performance of the SPRT over the fixed tool in the machining of titanium with appropriate cutting inserts. Flank wear exceeding 0.3mm was the reference for tool life during the fixed cutting tests as there were no catastrophic failures before reaching this state. This could be the result of protection provided on the rake face from material deposits

(further leading to a BUE), and the majority of material removal from the tool was along the flank wear land over the cutting distance.

During the self-propelled rotary tool cutting tests, material deposit was also observed along the circumferential rake face, but was considerably less than that developed on the fixed insert. Little to no crater wear was observed which can be attributed to the material deposits and significant reduction in heat generation along the cutting edge. Under the higher feed rate (0.3mm/rev), several local failures were observed on the insert (notching) during the intermediate stages of cutting until catastrophic failure at a particular site on the cutting edge was observed. This is believed to be the cause of the cyclical thermal shocking during machining with the rotating cutting edge. The carbide insert's mechanical properties were likely distorted due to the rapid increase and decrease in temperature along the cutting edge until they finally yielded and fracture occurred at a particular site. Given the observations of tool wear in the machining of Grade 5 titanium were very similar for both fixed and rotating conditions, the improvement in tool life by the SPRT can be largely attributed to the longer effective cutting edge provided by the tool rotation. Therefore, the improvement of tool life is expected to be proportional to the ratio between the circumference of the tool to the instantaneous contact arc length between the tool and the workpiece.

For all cutting tests it was observed that lowering the feed rate prolongs tool life; largely contributed to the decrease in cutting forces and relative velocities.

4.2 Characteristics of Tool Speed

It is apparent from the results collected in Figure 4.3 how the progression of flank wear affects the tool speed of the SPRT. During the initial break-in period of the tool (time from virgin cutting edge to development of flank wear), the tool average rotational speed decreases slightly from the first contact pass before it increases again and finds a steady rotational speed range. The possible reasons for such observations could include the following mechanical scenarios. Initial higher rotational speeds are the result from higher frictional forces generated by deglazing of surface impurities leftover from the edge honing process. The decrease in tool rotational speed is directly related to a decrease in the coefficient of friction as a result of oxidation layers forming on the virgin cutting edge. Once the conditions for generation of oxidation layers diminish, the frictional forces increase due to higher wear of the carbide substrate surface and thus increase tool rotational speed. Once the break-in period of the insert has been achieved, a steady range of tool speed will occur. It should be noted here that in addition to the cutting conditions, the tribology of the SPRT assembly will also affect the rotational speed of the tool. Therefore, it is assumed there is a very small loss in rotational tool speed as a result of friction in the bearings.

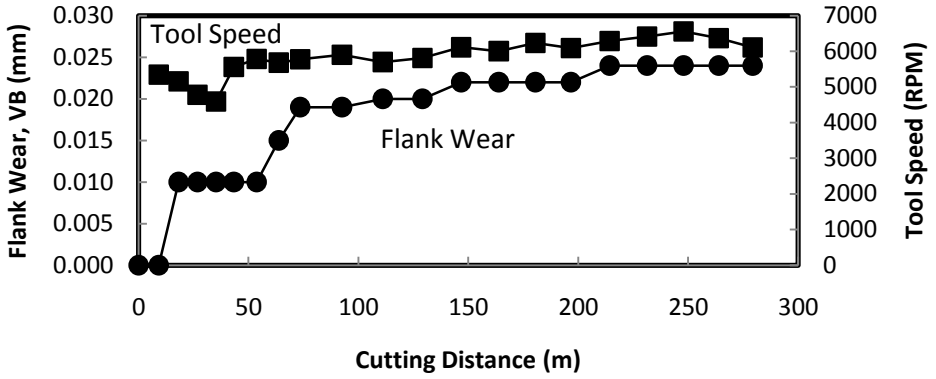

(a)

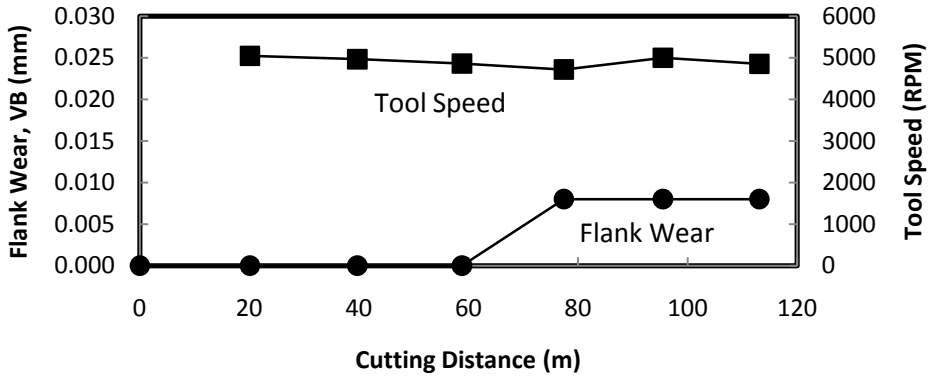

(b)

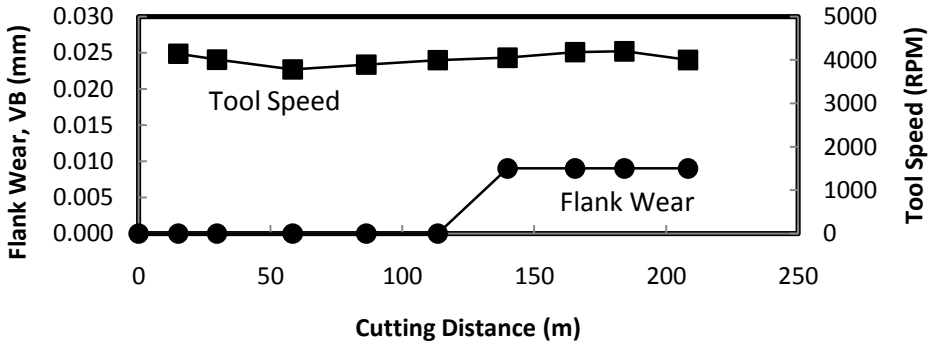

(c)

Figure 4.3 Flank wear progression and effect on tool speed during machining of AISI 4140 Steel for various feeds (V_w = 280 m/min, d = 0.3mm, feeds; (a) 0.3mm/rev, (b) 0.225mm/rev, (c) 0.15mm/rev, 9.5mm carbide insert).

As shown in Figure 4.4 below, tool rotational speed during the machining of titanium remained relatively constant over the entire cutting distance. The steady state rotational speed range is encountered immediately given there is no speed fluctuation during a break-in period at the initial stages of cutting as seen with the AISI 4140 steel machining tests. In fact, as shown by the flank wear progressions, tool wear occurs very rapidly (more noticeably at the higher feed rates), as a result of titanium's 'difficult-to-cut material' properties. Although a break-in period will have occurred, it happened too rapid to observe during data collection. There is however a similar tool break-in and rotational speed relation during the machining test with feed rate of 0.150mm/rev (Fig. 4.4 (c)), before the tool wear reaches a state where a steady speed range is observed.

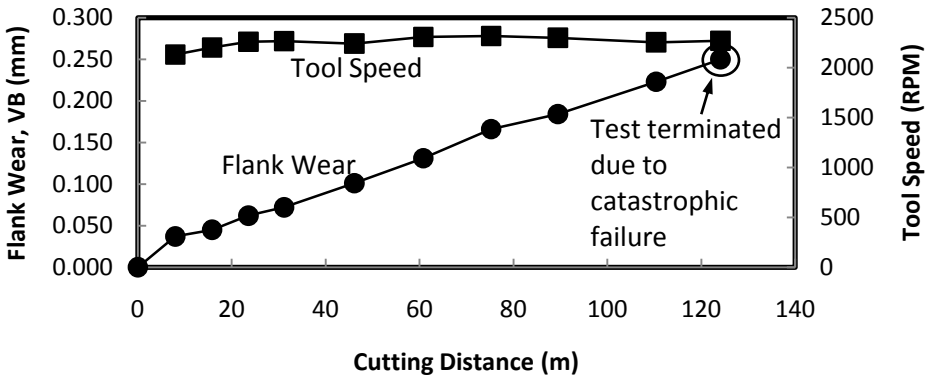

(a)

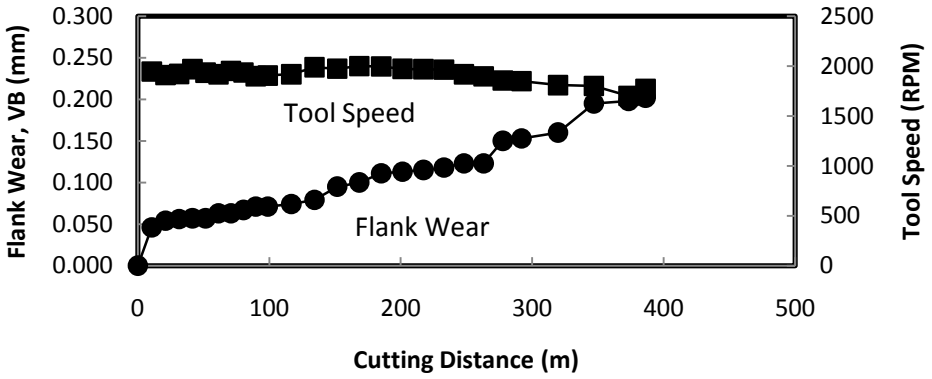

(b)

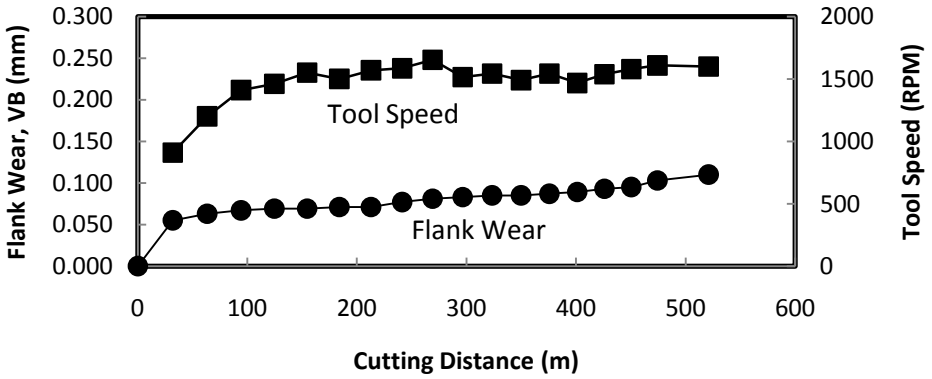

(c)

Figure 4.4 Flank wear progression and effect on tool speed during machining of Grade 5 Titanium for various feeds (V_w = 200 m/min, d = 0.2mm, feeds; (a) 0.3mm/rev, (b) 0.225mm/rev, (c) 0.15mm/rev, 9.5mm carbide insert).

As shown in Figure 4.5, an increase in feed rate produces an increase in average SPRT rotational speed for both materials tested. Given the tool cutting edge inclination angle was fixed and the cutting speeds and depths of cut were held constant for each material, the remaining cutting condition of feed rate shows a direct relation to tool speed. It should be noted here that the tool speeds plotted are the averages over the entire cutting distances. Although cutting conditions were relatively close for both materials, the differences in tool speeds can also be accounted for by the differences in abrasion wear, material deposition, and frictional losses.

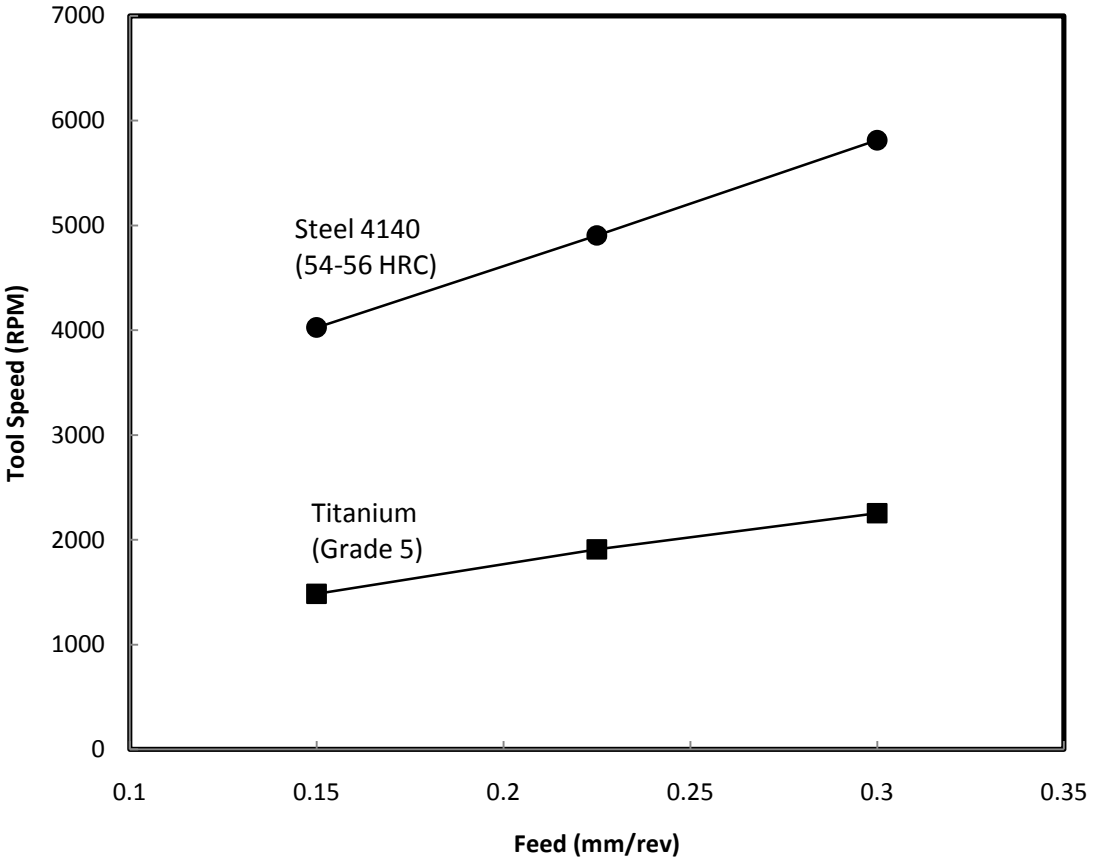

Figure 4.5 SPRT rotational tool speed during machining of different materials at different feed rates (AISI 4140 Steel: V_w = 280m/min, d = 0.3mm; Titanium (Grade 5): V_w = 200m/min, d = 0.2mm, 9.5mm carbide insert).

4.3 Characteristics of Surface Quality

Surface quality is an important factor that affects the performance of the mechanical component. The quality of the produced surface is strongly affected by the tool wear and the force generated. The assessment of the surface quality produced by the prototype SPRT with carbide insert is presented here.

Surface finish can be specified in a couple of ways; the peak-to-valley height and the center-line-average value. The peak-to-valley height is the root-to-crest value of roughness. The center-line-average value is based on a mathematical concept and is found by averaging the heights of the surface above and below a center line. The center line is a line parallel to the general direction of the profile such that the areas of the profile above and below the center line are equal. The values of surface roughness obtained in this investigation are all center-line-average values (Ra).

Figure 4.6 shows the surface roughness values measured on the hard turned surface produced by both the fixed tool configuration and self-propelled rotary tool with different feed rates. As shown, the fixed inserts have a smaller overall range in surface roughness values when compared to the range produced with the SPRT. However, at feed rates of 0.15mm/rev and 0.225mm/rev, the SPRT produces minimal difference in surface roughness values when compared to the fixed tool. Also, one can say that the SPRT produced cuts with roughness values within very reasonable limits. The larger difference observed between the SPRT and fixed tool at a feed rate of 0.3mm/rev, can be the result of several possible factors. Machine stability without a doubt plays a significant roll. The relative cutting velocity vector also affects the performance, which as shown earlier, is the result of the increased tool speed with feed (Figure 4.5). The moving parts and tribology of the SPRT assembly could also affect the acoustics of the cutting operation.

Similar results were also found during the machining of Grade 5 titanium as illustrated in Figure 4.7 below. However, a much larger difference in surface roughness is observed at a feed rate of 0.3mm/rev, which could be greatly influenced by the increased smearing action observed between the tool and workpiece. In addition, material sticking/welding on the workpiece was also much more substantial at this feed rate.

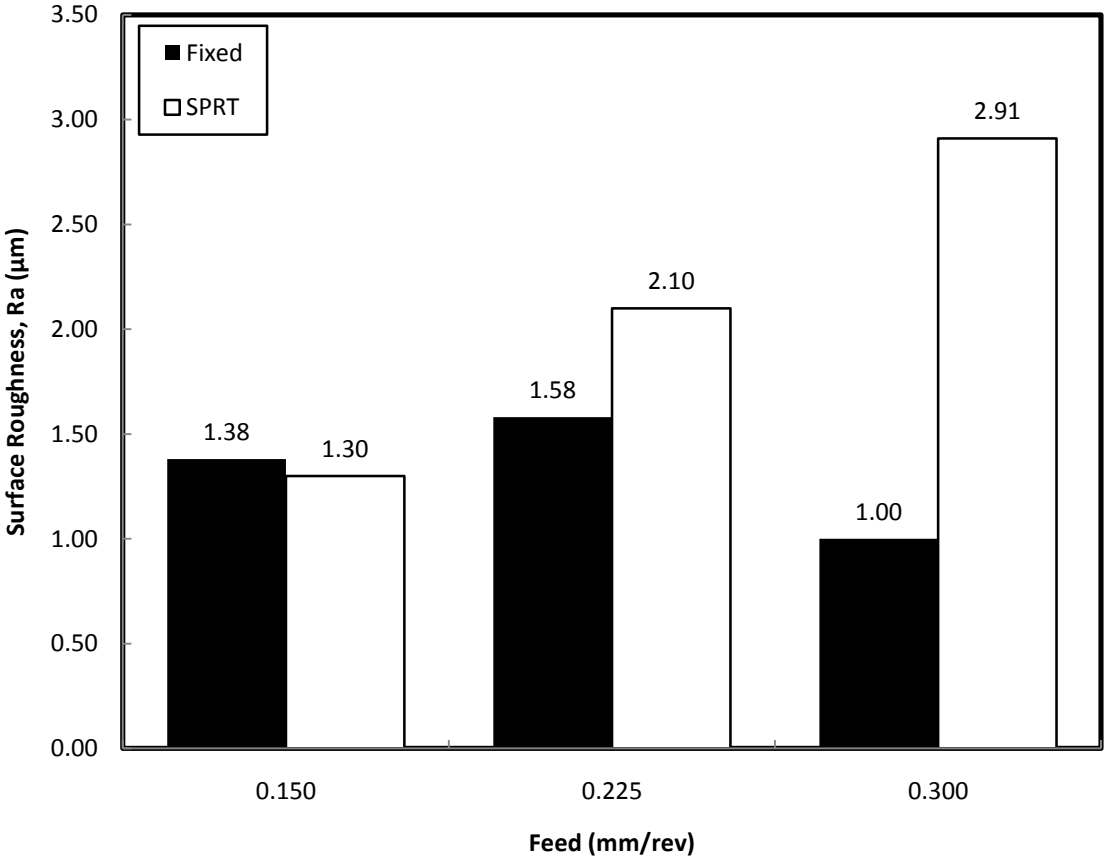

Figure 4.6 Surface roughness measurements during machining of AISI 4140 Steel at different feed rates (V_w = 280 m/min, d = 0.3mm, 9.5mm carbide insert).

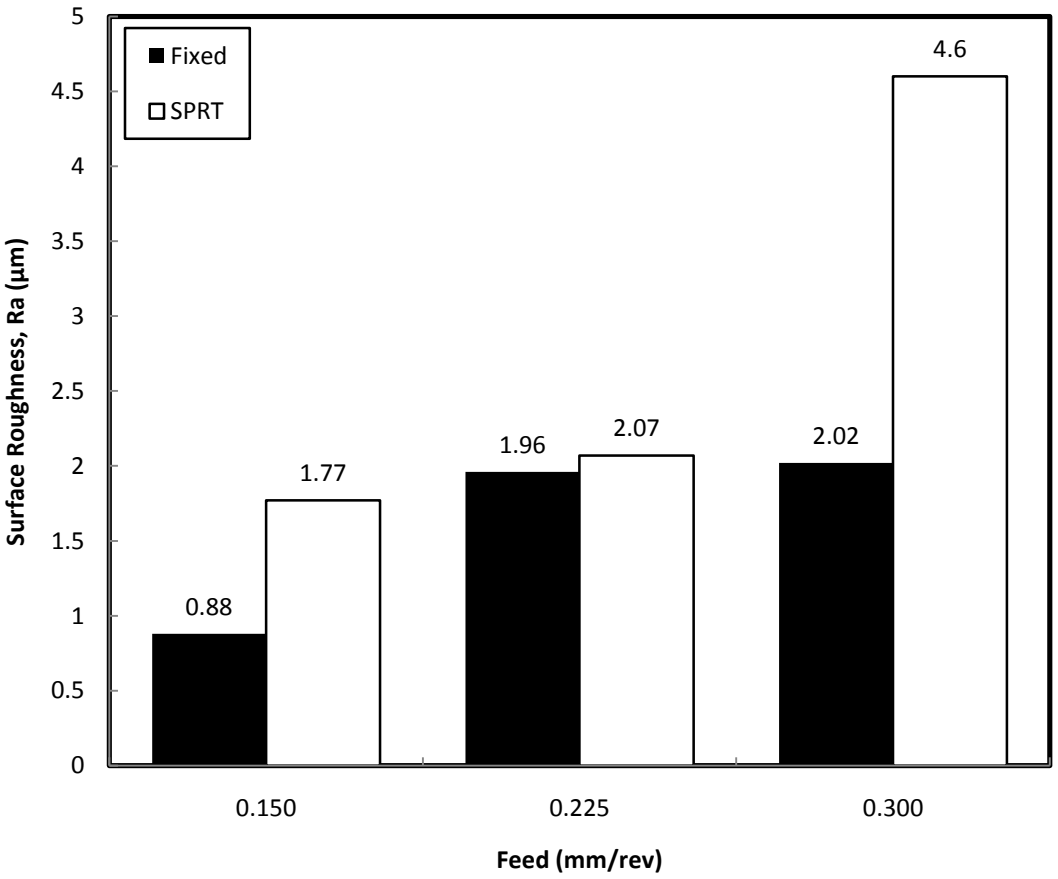

Figure 4.7 Surface roughness measurements during machining of Grade 5 Titanium at different feed rates (V_w = 200 m/min, d = 0.2mm, 9.5mm carbide insert).

Another observation made was the surface markings left on the machined surfaces of the SPRT hard turned materials. As shown in Figure 4.8 below, there is a cutting trace line indicated on the surface of machined titanium workpiece. The line is approximately measured to illustrate the direction of the markings. Clearly, contrary to the machined surfaces generated under conventional turning

and those generated by the fixed tool used in this thesis, the cutting trace lines typically coincide with the cutting direction. The trace line angles produced by the SPRT in this thesis, as shown in Figure 4.8, are smaller than the inclination angle of the tool (i = 25º) due to the existence of friction in the bearing assembly and the influence of relative cutting velocity.

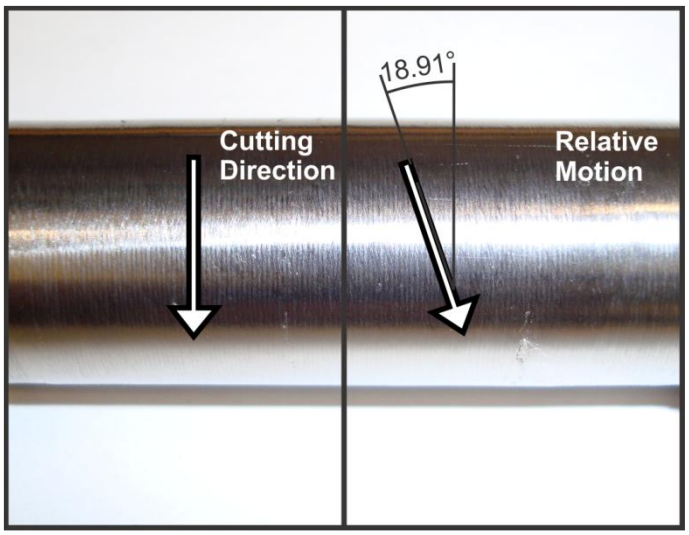

Figure 4.8 Trace lines generated on the surface of a SPRT hard turned Grade 5 Titanium workpiece sample (V_w = 200 m/min, d = 0.2mm, f = 0.225mm/rev, 9.5mm carbide insert).

4.4 Chip Formation Characteristics

From Figure 4.9 and Figure 4.10 below, the formation of chips during the machining of AISI 4140 steel and Grade 5 titanium with both the SPRT and fixed

tool are shown for different feed rates. For the steel machining tests, the curl radius of the spiral chips formed with the SPRT remained consistent and the smallest pitch was at the highest feed rate. All chips were segmented and discontinuous and the higher feed rate chips were approximately double the length of the lower feed rate chips. When comparing to the chips formed by the fixed tool during machining of steel, where the only difference in tools was the ability to rotate, it can be clearly seen how the rotational speed of the tool allows for helical chip formation. In addition, all chips formed by the fixed tool during machining of steel were continuous, which generates a safety hazard for the machinist and a source for surface damage during machining. The colour of the chips from the fixed tool tests (deep blue), are also an indicator of the much higher cutting temperatures generated compared to those from the SPRT tests (chips have no blue colouration).

Similarly for hard turning tests of Grade 5 titanium, the SPRT produced discontinuous segmented helical chips at all feed rates with almost equal curl radii and pitch dimensions. With the tool fixed, helical chips were formed with the increase in feed rates, and at 0.3mm/rev the chip formed is nearly identical to those produced by the SPRT. Also, the only discontinuous chip formed for fixed cutting tests was at the highest feed rate. It should be noted the continuous chips were cut for photo purposes.

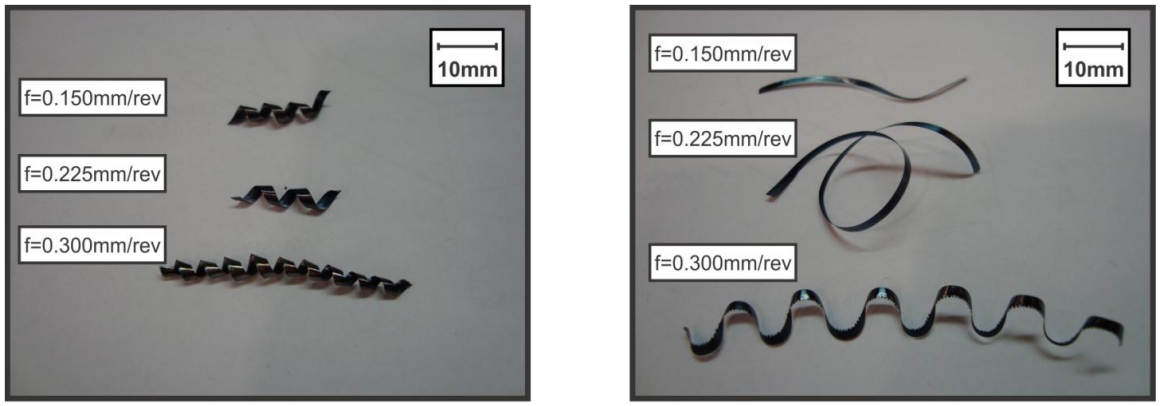

SPRT Fixed Tool

Figure 4.9 Typical chips obtained under different feeds during cutting of AISI 4140 Steel with SPRT and Fixed tool (V_w = 280 m/min, d = 0.3mm, 9.5mm carbide insert).

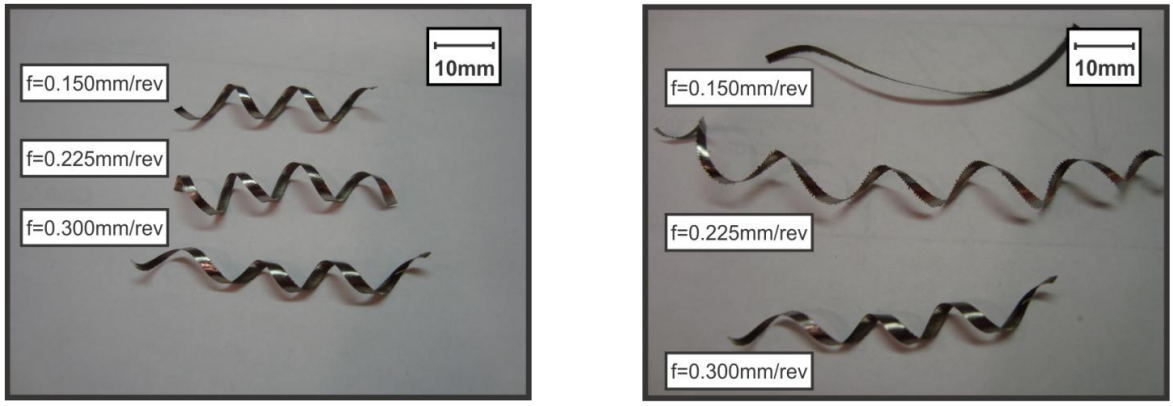

SPRT Fixed Tool

Figure 4.10 Typical chips obtained under different feeds during cutting of Grade 5 Titanium with SPRT and Fixed tool (V_w = 200 m/min, d = 0.2mm, 9.5mm carbide insert).

CHAPTER 5

CONCLUSIONS & FUTURE WORK

5.1 Summary

In this investigation, a self-propelled rotary tool (SPRT) was designed, prototyped, tested, and compared to a fixed tool with similar configuration. The results obtained meet the designed intent of the SPRT and validate the characteristics and benefits of these types of tools. The fixed tool produced better surface quality compared to the SPRT, however the differences are minimal and acceptable. When cost is considered, not only do the benefits of the SPRT obtained during machining make it economical, but the design of the prototyped tool also provides additional economical gains through maintenance, assembly, flexibility, and operation, especially when compared to the commercially available SPRTs for hard turning.

5.2 Conclusions

The main conclusions of this work can be summarized as follows:

1. The self-propelled rotary tool for hard turning achieved superior tool wear resistance and extraordinary improvement in tool life, relative to a fixed

tool with identical configuration and cutting conditions, when machining difficult-to-cut hardened steel and titanium workpiece materials.

2. Surface roughness values increased with feed rates for the SPRT which could be attributed to machine stability, smearing and material sticking, and acoustical interactions between the rotating bearing assembly and turning workpiece. It is not believed the higher surface roughness values are a result of inadequate tool rigidity or eccentricity of the rotating assembly.
3. Evenly distributed tool wear was observed along the circumference of the rotary tool inserts and there was minimal crater wear. Chipping or notching appeared to be the dominant failure mode when machining with the SPRT due primarily to thermal and mechanical shock induced by the continuous shifting of the tool edge during machining. In addition, material sticking/welding on the workpiece also promoted chipping of the SPRT insert.
4. Chip formation during machining with the SPRT was as per the intent of the tool design. In particular, the chips were helical with small pitch dimensions, and were discontinuous and segmented. This reduces the safety and machined surface problems associated with continuous chip formation.
5. Lower cutting temperatures associated with SPRTs were also observed during the machining tests (visually), which lowers the generation of

plastic deformation and surface hardness alterations in the workpiece material.

6. The effect of feed rate and SPRT rotational speed were also found to be directly related.

5.3 Recommendations for Future Work

It is suggested that future work regarding this type of machining be directed toward the following details:

1. Improvement to surface quality by self-propelled rotary tools, in particular reducing machine vibrations possibly caused by acoustics of the rotating assemblies.
2. Adapting the prototyped tool assembly to other machining processes and tool designs to gain economical benefits throughout the entire machining industry.

REFERENCES

[1] M. C. Shaw, P. A. Smith and N. H. Cook, 1952, “The Rotary Cutting Tool,” Transactions of the ASME, pp. 1065-1076.

[2] G. R. Nagpal, 1999, “Machine Tool Engineering,” Khanna Publishers.

[3] P. L. B. Oxley, 1989, “The Mechanics of Machining: An Analytical Approach to Assessing Machinability,” Ellis Horwood Limited, New York, NY.

[4] V. P. Astakov, 1998, “Metal Cutting Mechanics,” CRC, Boca Raton, USA.

[5] V. P. Astakov, 2008, “Tools (Geometry and Material) and Tool Wear,” in Machining: Fundamentals and Recent Advances, J. P. Davim, Portugal, Springer, pp. 29-57.

[6] V. P. Astakov, 2006, “Tribology of Metal Cutting,” Elsevier: London.

[7] E. Isakov, 2004, “Engineering Formulas for Metal Cutting,” Industrial, New York, NY.

[8] F. Klocke and T. Krieg, 1999, “Coated Tool for Metal Cutting – Features and Applications,” Annals of CIRP 48: Vol. 48, pp. 515-525.

[9] E. D. Whitney, 1994, “Ceramic Cutting Tools. Materials, Development and Performance,” Noyes, Westwood, NJ.

[10] “Modern Metal Cutting: A Practical Handbook,” Sandvik Coromart.

[11] “Tool-life Testing with Single Point Turning Tools,” ISO 3685:1993.

[12] F. W. Taylor, 1907, “On the Art of Cutting Metals,” Transactions of the ASME 28: pp. 31-58.

[13] E. M. Trent and P. K. Wright, 2000, “Metal Cutting,” Butterworth-Heinemann.

[14] M. R. Merchant, 1945, “Mechanics of the Metal Cutting Process. I. Orthogonal Cutting and a Type 2 Chip,” Journal of Applied Physics, Vol. 16, pp. 267-275.

[15] Y. Altintas, 2000, “Mechanics of Metal Cutting,” in Manufacturing Automation: Metal Cutting Mechanics, Machine Tool Vibrations, and CNC Design, Cambridge, UK. Cambridge University Press, pp. 4-65.

[16] H. A. Kishaway and M. A. Elbestawi, 1999, “On the Characteristics of Chip Formation in Hard Turning,” Proceedings of the 7th International

Symposium on Plasticity and its Current Applications (PLASTICITY '99"), pp. 361-364.

[17] K. Nakayama, M. Arai and T. Kanda, 1988, "Machining Characteristics of Hard Materials," Annals of CIRP – Manufacturing Technology, Vol. 37/1, pp. 89-92.

[18] P. Chen, 1991, "Characteristics of Self-Propelled Rotary Tools in Machining High Performance Materials," International Journal of Japan Society of Precision Engineering, Vol. 25/4, pp. 267-272.

[19] M. L. Penalva, M. Arizmendi, F. Diaz and J. Fernandez, 2002, "Effect of Tool Wear on Roughness in Hard Turning," Annals of CIRP, Vol. 51/1, pp. 57-60.

[20] V. Karri, 1991, "Fundamental Studies of Rotary Tool Cutting Processes," Ph.D. Thesis, University of Melbourne.

[21] V. A. Zemlyanskii and Y. F. Granin and B. V. Starchenko, 1962, "Circular Self-Rotating Tools," PNPTO Obrabotka Metallov Rezanlem, Vol. 1.6, No. M-62-71/10, Gosinti.

[22] V. A. Zemlyanskii, 1965, "Wear of Circular Self-Rotating Tools Expressed as a Function of the Length of Path of Travel on the Cutting Edge on the Workpiece," Samoletostroenie I Technika Vozdushnogo Flota, Part 3, pp. 86.

[23] V. A. Zemlyanskii, 1963, "Kinematics of Machining with Self-Rotating Tools," Samletostroenie I Tekhnikha Vozdushnogo Glota, Part 1, pp. 112.

[24] V. A. Zemlyanskii and Y. F. Ganin, 1965, "Dynamic Investigations on Circular Self-rotating Tools," Izvestia Visshik Uchebnikzavednii Mashinostroenic, Part 1.

[25] V. A. Zemlyanskii, 1965, "On the Problem of Increasing the Productivity of Machining," Samolestostroenic I Technika Vozdushnogo Flota, Part 1, pp. 104.

[26] V. A. Zemlyanskii and Y. F. Ganin, 1965, "Circular Self-Rotating Tools," Mashinostroitel, Vol. 6, pp. 35.

[27] V. A. Zemlyanskii, 1965, "Investigation on the Three Dimensional Deformation of Metal White Machining with a Circular Self-Rotating Tool," Samoletostroenie I Technika Vozdushnogo Flota, Kharkov Part 2, pp. 98.

[28] V. A. Zemlyanskii, 1966, "Method of Analyzing the Kinematics of Circular Self-Rotating Tools," Stanki I Rezh. Instrumentu, Resp. Mezhved, Nauchno Tekhn Sbornik, Vol. 2, pp. 19.

[29] V. A. Zemlyanskii,1966, “Cutting Speeds While Machining with Circular Self-Rotating Tools,” Stank Ii Rezh. Instrumentu, Resp. Mezhved, Nauchno Tekhn Sbornik, Vol. 2, pp. 43.

[30] V. A. Zemlyanskii, 1966, “Self Induced Rotation of Round Tool Tips,” Russian Engineering Journal, Vol. 156, No. 9, pp.66.

[31] Y. F. Ganin, 1963, “Investigation on the Longitudinal Chip Reduction While Machining with Self Rotating Tools,” Trudi Kharkovskogo Aviatsonnogo Instituta, No. 14-63-762/33.

[32] Y. F. Ganin, 1965, “Wear and Life of Circular Self Rotating Tools,” Samoletostronie I Teknika Vozdushnova Flota, Vol. 2, pp. 106.

[33] I. S. Kooshner, 1962, “Investigations on the Turning Process While Working with Circular Self-Rotating Tools,” Sb.Obrabativaemost Zharaprochnikh I Titaovikh Splavov, Trudi Vessoyuznoi Mezhvuzovski Konferentsii, Kuibishev, pp. 218.

[34] I. S. Kooshner, 1963, “Circular Self Rotating Tools with Long Life in Turning,” PNPTO, Izd-Vo-KHGU, Vol. 22, No.14-63-762/33.

[35] A. N. Reznikov, 1962, “Theoretical Fundamentals About Active Cooling of Tools,” Sb.Obrabativaemost Zharaprochnikh I Titaovikh Splavov, Trudi Vessoyuznoi Mezhvuzovski Konferentsii, Kuibishev, pp. 247.

[36] A. N. Reznikov and I. S. Kooshner, 1962, “Tools with Great Potentials,” Promishlenno Ekonomicheskoi Bulletin, Kuibshev, pp. 247.

[37] A. N. Reznikov and V. V. Ledyayev, 1966, “Rubbing on the Flank Surface of Cutting Tools While Turning with Deliberately Rotated Circular Tools,” Izvestia Visshik Uchebnik Zavednii Mashinostroenic, No. 1, pp. 170.

[38] E. G. Konovalov and I. L. Tarakanov, 1966, “Cutting with Self Rotating Cutters,” Dokladu Akad, Nauk BSSR, Vol. 10/11, pp. 849.

[39] E. G. Konovalov and I. L. Tarakanov, 1967, “Investigations on Cutting with Spontaneous Tool Rotation,” Izvestia Akad, Nauk, Vol. 3, pp. 52.

[40] V. C. Venkatesh, S. Rajesham and V. Kamala, 1972, “Wear and Surface Finish in Face Milling with Rotary Inserts,” 5th All India MTDR conference, Roorkee, pp. 183.

[41] P. Chen, 1992, “High Performance Machining of SiC Whisker-reinforced Aluminum Composite by Self-Propelled Rotary Tools,” CIRP, STC C, Vol. 41/1, pp. 59-62.

[42] H. A. Kishawy, A. M. Shawky and M. A. Elbestawi, 2001, “Assessment of Self-Propelled Rotary Tools During High Speed Face Milling,” 4th

International Machining & Grinding Conference, MR01-227, Troy, Michigan, USA, pp. 1-10.

[43] H. A. Kishawy and A. G. Gerber, 2001, “A Model for Tool Temperature During Machining with a Rotary Tool,” ASME International Mechanical Engineering Congress and Exposition, New York, NY, IMECE2001/MED-23312, pp. 1-8.

[44] V. Dessoly, S. N. Melkote and C. Lescalier, 2004, “Modelling and Verification of Cutting Tool Temperatures in Rotary Tool Turning of Hardened Steel,” International Journal of Machine Tools & Manufacture, Vol. 44, pp. 1463-1470.

[45] Y. Zhang, J. Wilcox and H. A. Kishawy, 2003, “An Assessment of Carbide Self-Propelled Rotary Tools During Machining of Hardened Steel,” NAMRI/SME 31st North American Manufacturing Research Conference, Hamilton, Ontario, Canada, pp. 185-192.

[46] S. Lei and W. Liu, 2002, “High-speed Machining of Titanium Alloys Using the Driven Rotary Tool,” International Journal of Machine Tools & Manufacture, Vol. 42, pp. 653-661.

[47] E. J. A. Armarego, V. Karri and A. J. R. Smith, 1993, “Computer-aided Predictive Models for Fundamental Rotary Tool Cutting Processes,” Annals of the CIRP, Vol. 42/1.

[48] E. J. A. Armarego, V. Karri and A. J. R. Smith, 1994, “Fundamental Studies of Driven and Self-Propelled Rotary Tool Cutting Process – II. Experimental Investigation,” International Journal of Machining Tools & Manufacturing, Vol. 34, No. 6, pp. 803-815.

[49] E. J. A. Armarego and R. K. Katta, 1997, “Predictive Cutting Model for Forces and Power in Self-Propelled Rotary Tool Turning Operations,” Annals of the CIRP, Vol. 46/1.

[50] L. Li, 2005, “A Force Model for Self-Propelled Rotary Tools,” MASc. Thesis, University of New Brunswick.

[51] V. A. Zemlyanskii and V. Lubking, 1983, “The Machining of High Speed Materials Using Self-Propelled Rotary Cutting Tools,” National Defence Industry Press.

[52] British Standard Instituion, 1972, “Specification for Single Point Cutting Tools, Part 2, Nomenclature,” BSI1296: Part 2.

[53] E. J. A. Armarego, V. Karri and A. J. R. Smith, 1994, “Fundamental Studies of Driven and Self-Propelled Rotary Tool Cutting Processes – I. Theoretical Investigation,” International Journal of Machine Tools & Manufacturing, Vol. 34/6, pp. 785-802.

[54] W. Y. Chen, 1993, “The Machining of Hardened Steel Using Superhard Tooling CBN and CBN Tipped Rotary Cutting Tool,” Ph.D. Thesis, University of Birmingham.

[55] A. H. Bekkala and C. H. Kahng, 1979, “A Study on the Self-Propelled Rotary Tooling,” Manufacturing Engineering Transactions, 7th NAMRC, pp. 255-261.

[56] A. A. Radwan, 1981, “Shear Angle Relationship in Cutting with Self-Propelled Rotary Tool,” SME Manufacturing Engineering Transactions, 9th NAMRC, pp. 437.

APPENDIX

Appendix A: Insert Properties

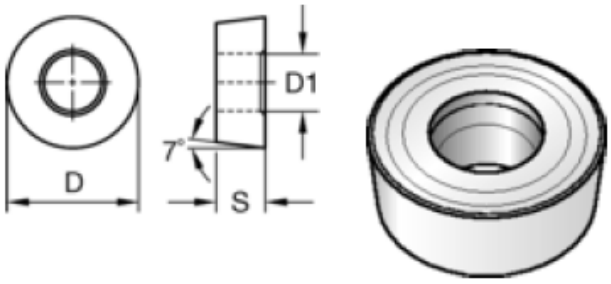

■ RCMT

		D		L10		S		Rε		D1		
ISO catalog number	ANSI catalog number	mm	in	mm	in	mm	in	mm	in	mm	in	ANSI catalog number
RCMT09T300	RCMT325	9,53	3/8	-	-	3,97	5/32	-	-	4,40	.173	RCMT325

Uncoated Carbide Grades	**K313**	 C3 – C4	**composition:** A hard, low binder content, unalloyed WC/Co fine-grained grade. **application:** Exceptional edge wear resistance combined with very high strength for machining titanium, cast irons, austenitic stainless steels, non-ferrous metals, nonmetals, and most high-temperature alloys. Superior thermal deformation and depth of cut notch resistance. The grain structure is well controlled for minimal pits and flaws, which contributes to long, reliable service.
	KC5010	 C3	**composition:** A hard, low binder content, unalloyed grade WC/Co fine-grained grade. **application:** The K68 grade has excellent abrasion resistance for machining cast irons, austenitic stainless steels, non-ferrous metals, nonmetals and as an alternative to the K313 grade on most high-temperature alloys. Use as a general purpose grade for non-ferrous materials.

NOTE: Grade of insert used was KC5010
Source/Manufacturer: Kennametal©

Appendix B: Self-Propelled Rotary Tool Design

The design intent of the developed self-propelled rotary tool is to bring to the machining industry what the two currently manufactured SPRTs for hard turning lack in terms of affordability and flexibility, while achieving the performance benefits of SPRTs. Currently, both Rotary Technologies© and Mitsubishi Materials© offer a SPRT for hard turning processes. Each company's design is comprised of their own proprietary components (i.e. inserts, bearing assemblies, seals, hardware, etc.). As a machinist or manufacturing facility, this leaves limited resources to maintain operation and serviceability of these tools on in economical fashion. Given the "one-off" designed components of these tools, both Rotary Technologies© and Mitsubishi Materials© can demand higher costs given their limited market competition. In addition, both self-propelled rotary tool designs have complex assemblies that make serviceability/maintenance of the tool more complicated.

Rotary Technologies© SPRT for hard turning utilizes simple disk inserts with a cutting edge diameter of 25.4 mm, however they are not standard ISO inserts readily available from other tool manufacturing companies. The inside diameter of the insert makes the geometry of the tool proprietary to Rotary Technologies© SPRT. Similarly, Mitsubishi Materials© uses a 12.7 mm insert, but the geometry on the base of the insert (opposite the cutting edge) makes the tool unique compared to the ISO inserts commercially available. As discussed in this thesis, the use of large diameter inserts can result in improved surface

quality, however they can simultaneously generate larger thrust forces during machining which can lead to increased tool chatter if the machine tool is not sufficiently rigid. Both tool manufacturers offer the SPRT for hard turning with a fixed inclination angle *i*, and rake angle *α*, for the cutting edge. Both tools can machine workpiece materials of any diameter.

B.1 Tool Design

The following figures present the self-propelled rotary tool design and assembly. Following is the justification for the selection of the presented components and the assembly.

Part #	Description
1	M35x10 T15 Torx Screw
2	RCMT 09 T3 00 (9.5 mm insert)
3	Tool Support
4	Needle Roller Thrust Bearing
5	Needle Roller Bearing
6	Needle Roller Thrust Bearing
7	Thrust Washer
8	M8 Washer
9	M8 Nut
10	Tool Fixture

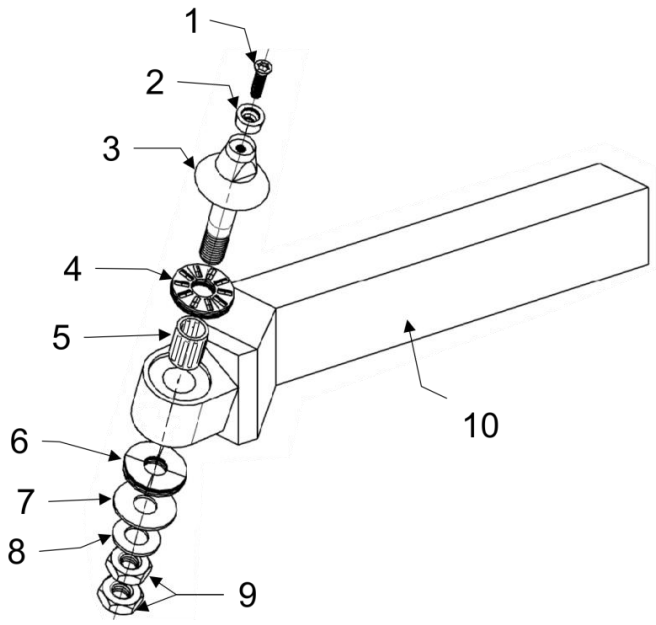

B.1 Self-propelled rotary tool assembly.

The first consideration for the tool design was the inclination angle for the cutting edge. Based on several studies on the effects of SPRT inclination angle and its effect on chip formation and cutting forces [1, 41, 48, 50], a tool inclination angle *i* of 25º was selected for the tool design. This configuration was found to provide significant reduction in cutting forces and thus machining power, while simultaneously generating discontinuous and segmented chips of difficult-to-cut materials. This chip formation also eliminates any workpiece surface damage caused by continuous chips which can become tangled around the workpiece and lathe chuck. In addition, the inclination angle also directs the discontinuous chips (which are both very hot and sharp) away from the machinist and towards the lathe bed. By similar desired characteristics, a cutting edge rake angle of -5º was found [1, 41, 48, 50] to provide the same results while generating improved surface quality of SPRT tools compared to larger positive rake angles. Thus, an inclination angle *i,* and rake angle α, were applied to the tool fixture (Part #10 in Figure B.1) such that the posture of the cutting insert would generate the aforementioned results.

A large factor in the development of the design and assembly of the remaining components revolves around the ability to do so with readily available 'off-the-shelf' components. This provides the economical benefits to the machinist since part replacement can be conducted easily through the use of any industrial supply outlet. This provides improved service/maintenance when compared to other commercially available SPRTs for hard turning. Development within the capabilities of the readily available components is the design of the tool

support (Part #3 in Figure B.1). The geometry of this component must accomplish the following:

1. Provide a method of clamping the insert such that the cutting edge is concentric with the rotational axis.
2. Provide sufficient strength/rigidity to absorb cutting forces and not result in ‘out-of-round’ rotation.
3. Provide enclosure of the bearing components that protects them from cutting elements; such as metal chips and/or powder.
4. Provide a method that allows assembly to the tool fixture (Part #10) while still permitting rotation of the component.
5. Provide assemblage that is not cumbersome or difficult for the operator to maintain and service, as well as provide quick and easy changing of cutting inserts.

Two requirements that are difficult to overcome are those listed as #2 and #3 above. Currently, the most readily available needle roller thrust bearings have a much larger outside diameter than the cutting insert (9.5 mm). A needle roller thrust type bearing is chosen since they require very narrow axial space and can maintain substantial axial loading. The former characteristic complements the second requirement (as listed above), since the tool support must fix the insert at a small axial height away from rotating assembly to minimize bending and deflection of the component caused by the cutting forces. Therefore, to fix the insert (of smaller diameter) and enclose a thrust bearing (of much larger diameter) negates tool support geometry similar to a frustum. Through

substantial market research, a needle roller thrust bearing with outside diameter of 21mm was selected. The difference in diameters from insert to bearing would generate a very tall frustum support geometry; hence the 'stepped' frustum design (shown in Figure B.1 and Figure B.2 below). This geometry has a small axial height between the insert and thrust bearing; thus minimizing bending moments compared to a non-'stepped' frustum geometry. Given the inclination and rake angles set by the tool fixture, the reduced axial height limits the range of machinable workpiece diameters. However, the primary application of the SPRT for turning is for automotive and powertrain-related components; shafts that are normally hard-to-cut materials and relatively small in diameter. Therefore, the height of the support that minimizes deflection, allows for workpiece diameters up to 38.1mm; the average diameter of automobile transmission input shafts, for example. The deflection criteria was based on the results from a simplified finite element analysis (FEA) of the SPRT assembly exposed dynamically to 1000 N (maximum cutting forces obtained in other works [41,50]) in the x, y, and z cutting force directions at a point on the cutting edge. The maximum deflection was approximately 0.2mm, which is minimal and results in reasonable runout when considering vibration and surface quality. Figure B.2 below illustrates the complete rotating assembly of the SPRT.

Part #	Description
1	M35x10 T15 Torx Screw
2	RCMT 09 T3 00 (9.5 mm insert)
3	Tool Support
4	Needle Roller Thrust Bearing
5	Needle Roller Bearing
6	Needle Roller Thrust Bearing
7	Thrust Washer
8	M8 Washer
9	M8 Nut
10	Tool Fixture

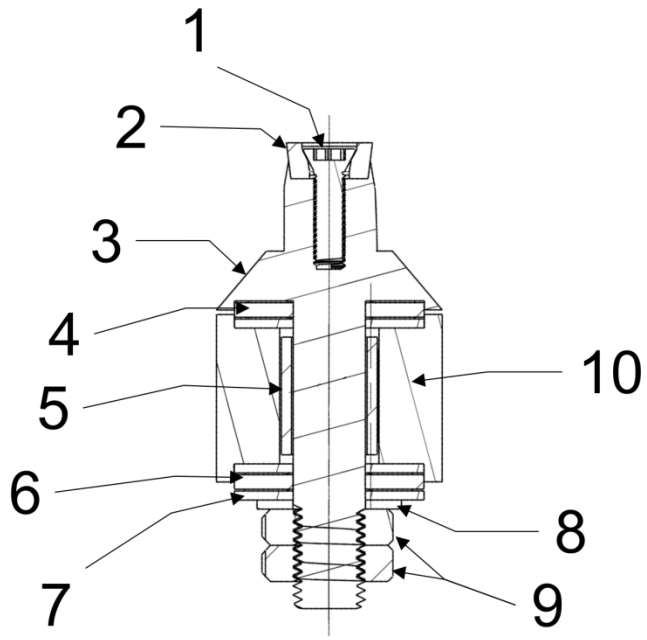

B.2 Self-propelled rotary tool rotating assembly.

As shown in Figure B.2, the tool support (Part #3) encloses the thrust bearing (Part #4) and maintains clearance with the tool fixture (Part #10) such that machined material cannot enter. This provides protection from possible damage to the bearing rollers, races, and cages. Below the thrust bearing (Part #4), a needle roller bearing (Part #5) is assembled to provide additional rotational freedom to the tool support. Given the thrust bearing is only capable of providing support in the axial direction, this needle roller (Part #5) is inserted to absorb the radial forces applied to the cutting insert and maintain concentric rotation. The tall needle rollers provide support along the majority of the surface of the tool

support (Part #3) that is surrounded by the tool fixture (Part #10). To maintain rigidity with the tool fixture, the bottom portion of the tool support is clamped with two jam-nuts, which eliminate any axial movement. A needle roller thrust bearing and thrust washer (Part #6 and #7) is also assembled between the jam-nuts and tool fixture to allow free rotation of the support. In addition, the insert is fixed concentrically in the support by a tapered pocket that conforms to the flank surface of the cutting insert. By this method the insert's outer circumference is used for centering the cutting edge which is more accurate than centrally locating the insert with the inner hole; degree of concentricity between the cutting edge and inner hole may not be true given the inserts are not originally designed for rotary cutting tools. The insert is seated in the tool support and a screw is used to clamp it. To provide ease of assembly, two parallel faces on the support are designed just below the insert, set a distance of 10mm apart, such that an ordinary wrench can be used to help torque the insert screw and the jam-nuts.

Therefore, the developed SPRT for hard turning provides simplicity in assembly, operation, and service/maintenance. There is no requirement for lubrication of the bearings since they are designed for dry working environments, however, if cutting fluids are used during the machining operation, they will not cause any damage to the components. Not including the tool support (Part #3) and the tool fixture (Part #10), all remaining parts are commercially available as 'off-the-shelf' components. In addition, currently this is smallest cutting insert diameter SPRT design. This provides the additional benefits to SPRTs by also

obtaining turned profiles closer to stepped geometrical designs (due to reduce cutting tool radius) while also reducing thrust cutting forces.

VITA

Full Name:	Grant Leonard Parker
Universities Attended:	University of Ontario Institute of Technology, B. Eng., Automotive Engineering, June 2009